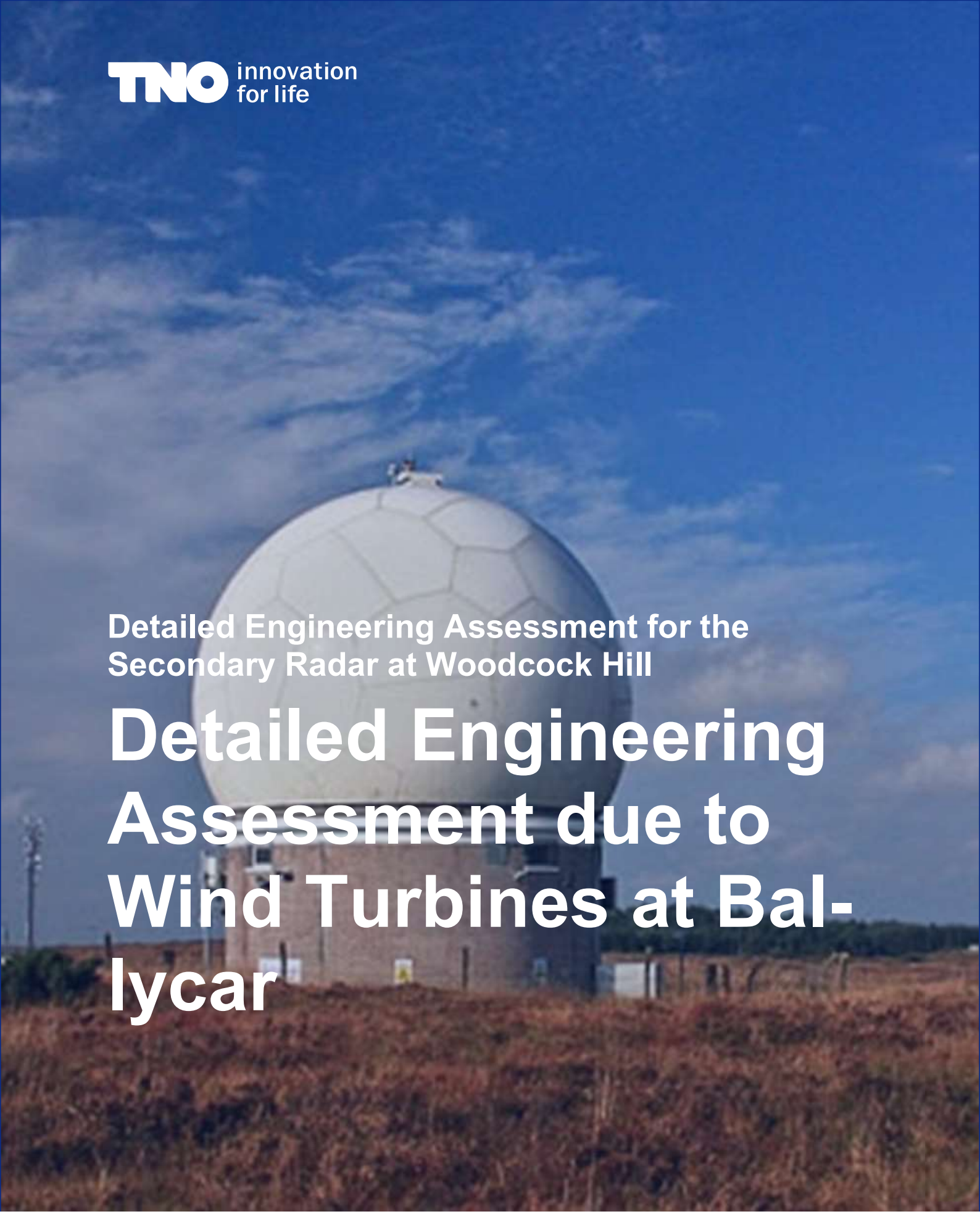

TNO innovation for life

Detailed Engineering Assessment for the Secondary Radar at Woodcock Hill

Detailed Engineering Assessment due to Wind Turbines at Ballycar

TNO Intern ⟩ TNO 2026 R10051

19 January 2026

Defence, Safety & Security
www.tno.nl
+31 6 46 96 60 46
perseus@tno.nl

TNO 2026 R10051 – 19 January 2026

Detailed Engineering Assessment due to Wind Turbines at Ballycar

Detailed Engineering Assessment for the Secondary Radar at Woodcock Hill

Author(s)	Onno van Gent, Detmer Bosma
Classification report	TNO Intern
Title	TNO Intern
Report text	TNO Intern
Number of copies	Number of copies
Number of pages	39 (excl. front and back cover)
Number of appendices	0
Sponsor	Ai Bridges Limited
Project name	DEA MSSR Woodcock Hill Ballycar
Project number	060.67849/01.03.01

Contents

Abbreviations

Abbreviation	Meaning
ACP	Azimuth Change Pulse
AGL	Above Ground Level
AFB	Air Force Base
AMSL	Above Mean Sea Level
ARB	Auxiliary Reference Burst
ASR	Airfield Surveillance Radar
CAGO	Cell Averaging Greatest Of
CFAR	Constant False Alarm Rate
CTR	Controlled Traffic Region
CUT	Cell Under Test
DEM	Digital Elevation Model
EGM96	Earth Gravitational Model 1996
LVA	Large Vertical Aperture
MRB	Main Reference Burst
MSSR	Monopulse Secondary Surveillance Radar
NASA	National Aeronautics and Space Administration
NGSP	Next Generation Signal Processor
OBE	Off-Boresight Error
PSR	Primary Surveillance
RCS	Radar Cross section
RPM	Revolutions Per Minute
SSR	Secondary Surveillance Radar
SRTM	Shuttle Radar Topography Mission
SWG	Slotted Wave Guide
TNO	Netherlands Organisation for Applied Scientific Research
VCC	Vertical Clutter Cancellation
WC	Worst-case
WT	Wind Turbine
WFF	Wind Farm Filter
WGS84	World Geodetic System 1984

1 Introduction

The performance of radar systems can be negatively influenced by wind turbines in their vicinity. EUROCONTROL has issued guidelines, on how to assess the potential impact of wind turbines [1]. Within these guidelines different zones around the radar are defined. A Detailed Engineering Assessment (DEA) for the primary radar is required at distances to the wind turbines ranging from 500 m to 15 km (zone 1). In the zone ranging from 15 km to the instrumented range of the primary radar (zone 2), a so-called Simple Engineering Assessment (SEA) is required in case there is line of sight. For the secondary radars, a DEA needs to be performed in case the wind turbines are located closer than 16 km from the radar.

Ballycar Green Energy Limited have plans to build the Ballycar Wind Farm comprising of twelve wind turbines. Ballycar Green Energy Limited has used the technical assistance of Ai Bridges Limited and the aviation specialists Cyrrus Limited. Following a presentation by TNO in November 2025 to Ballycar Green Energy Limited , Ai Bridges Limited and Cyrrus Limited. TNO were then commissioned to prepare a Detailed Engineering Assessment due to the Wind Turbines at Ballycar.
All wind turbines will have a tip height of 158 m. The closest wind turbine is located at a distance of approximately 2.5 km from the secondary radar at Woodcock Hill, so inside the 16 km distance from the radar. Therefore a DEA needs to be performed for the secondary radar following the EUROCONTROL guidelines.

In Section 2 the general information is given and in Section 3 the specific input parameters of the relevant wind turbines and radar for this study are given. In Section 4, we perform the DEA for the MSSR at Woodcock Hill. Finally, in Section 5 conclusions are drawn.

2 General Information

2.1 Effects of wind turbines on MSSR

The presence of wind turbines can influence the performance of MSSRs. In order to correctly interpret the results of the Line-of-Sight analysis, we address the most important issue that can arise whenever a wind farm is near a secondary radar system: bearing errors.
SSRs differ from PSRs in a number of ways. PSRs do not depend on cooperation of aircraft, they merely measure range, bearing and sometimes also elevation angle and radial velocity. SSRs demand that aircraft cooperate, *i.e.*, the aircraft actively participates in its detection. The SSR sends out an interrogation signal at 1030 MHz. The target, carrying a radar transponder, subsequently replies by transmitting a response signal at 1090 MHz. This response contains additional information regarding the target, *e.g.*, barometric altitude (mode C) and an identity code (mode A). In the case of monopulse SSR (MSSR), the system is capable of making a precise bearing estimate of the target from a single reply signal. The bearing estimate of this single reply is generally accurate within a fraction of a degree (~0.05°) and the larger the range to the target the more this angle error, off-boresight error or OBE, will translate in a cross-range error. The presence however of an obstacle (like a mountain, building or wind turbine) between the MSSR antenna and the target can cause an error in the estimation of the bearing to the target.

In Figure 2.1 an MSSR antenna is shown, typically comprising 35 antenna elements. Below we first give a short description on how the bearing measurement is carried out and how the wind turbine influences this measurement.

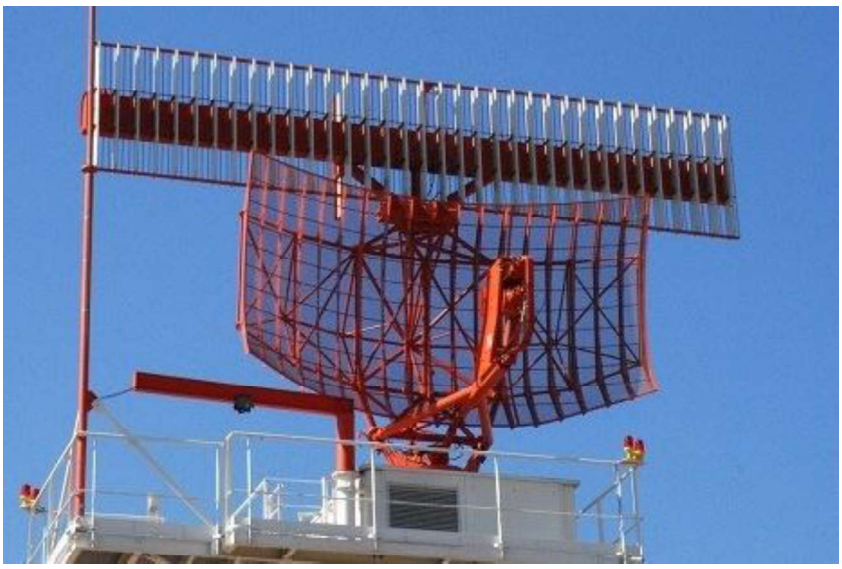

Figure 2.1 The secondary radar antenna, comprising of 35 antenna elements, on top of a STAR 2000 antenna.

The bearing to a target is determined using the so-called monopulse technique. By applying different weight factors for each antenna element, two radar beams are created with the same antenna, the so-called *sum beam* and *difference beam*, see Figure 2.2. A reply is received by both beams. By comparing the signal strength in the sum beam to the signal

strength in the difference beam an accurate bearing angle can be estimated. Left-right ambiguity is solved by looking at the phase of the signal. For example, when the sum and difference beam record a pulse with the same signal strength, looking at Figure 2.2 we see that the bearing to the target must be, depending on the phase, either +1° or -1°.

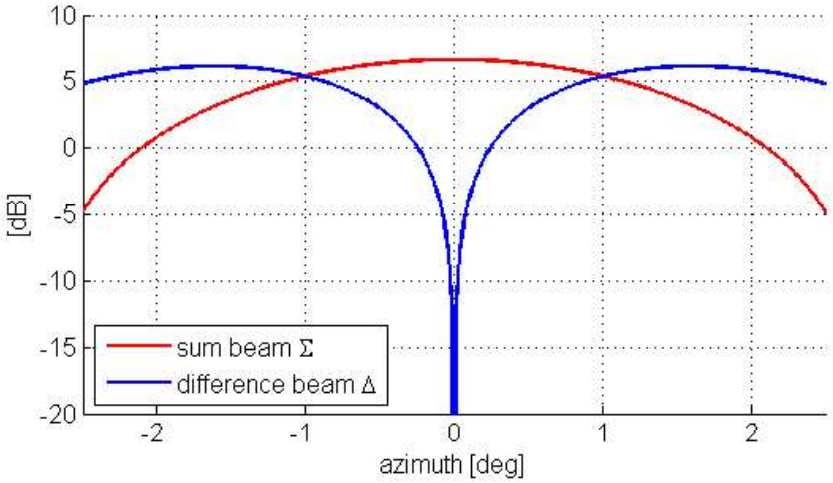

Figure 2.2 The sum beam (red) and difference beam (blue) used within the TNO model. The bearing of the target is estimated by comparing the signal strength of a single reply signal in both beams.

If a wind turbine is positioned between the target and the radar, the received electric field is distorted both in phase and in amplitude. This is illustrated in Figure 2.3. The distorted field effectively changes the weight factor at each antenna element, thus, changing the shape of the sum beam and difference beam. As the two beams are influenced differently by the wind turbine, so is the signal strength measured in both beams. Therefore, when the signal strength is compared to estimate the bearing, an error is introduced.

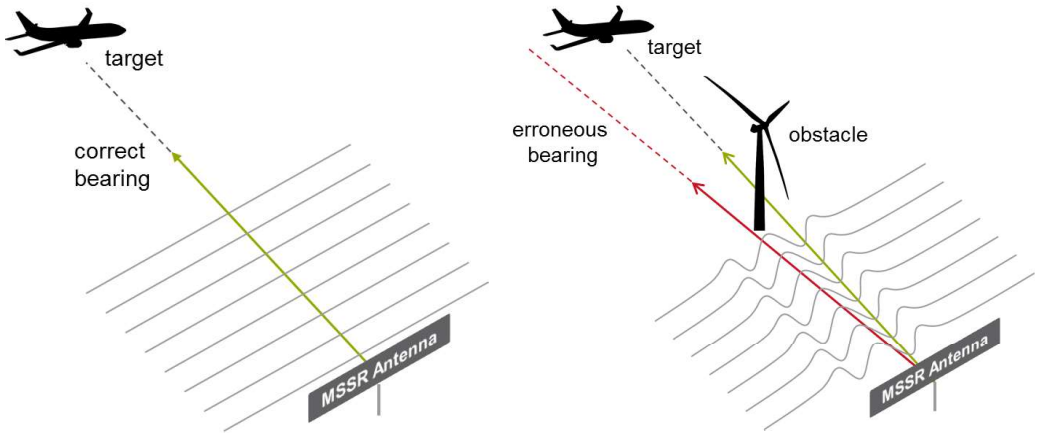

Figure 2.3 A wind turbine, positioned between target and MSSR antenna can disturb the transponder signal, introducing an error in the bearing estimate.

The bearing error as a function of azimuth angle to the target has been calculated. This will give us insight in the width of the zone in which the MSSR is influenced by the wind turbine. To estimate the bearing error we use an analytical solution for an incident plane wave on a cylinder with fixed radius and infinite length. The method calculates the phase and amplitude of the perturbed wave front on each antenna element. From this the bearing error is determined. The method is described in full in [2]. In this reference the method has been

validated using real data of an MSSR partially obstructed by a metal mast of width ~2 meter at a range of approximately 600 meter.

TNO has conducted its own validation of the method as well using real MSSR data. In this validation the MSSR is partly obstructed by an ATC tower with a maximum width of 20 meter at a range of approximately 2 km. In both cases, the calculated bearing error as a function of azimuth matched relatively well with the measured data. Figure 2.4 shows the close match between real recorded MSSR track of an aircraft at a distance around 175 km from the MSSR and the simulated data. Secondary effects at coordinates [4, 178] and [-4, 174] km appear accurately modelled as well (indicated by red arrows).

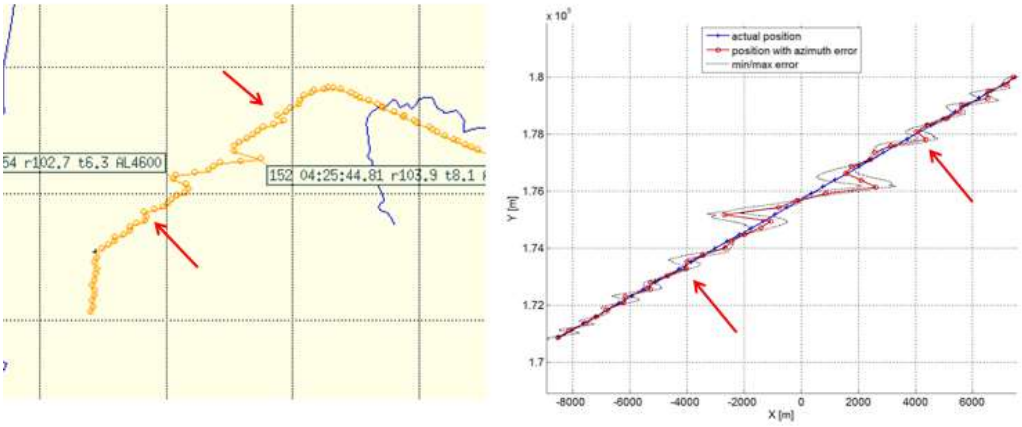

Figure 2.4 Comparison of a MSSR track recoding of a real aircraft and the simulated results. Secondary effects at coordinates [4, 178] and [-4, 174] km appear accurately modelled as well (indicated by red arrows).

As mentioned, the method uses a cylinder of infinite length to model the obstacle. An infinite cylinder can be described by just a single parameter, its width. In our simulations we have chosen the width of the cylinder to be dependent on whether or not the nacelle or blades can be seen by the radar, see Figure 2.5. In the orange sector, the width of the cylinder is equal to the average of the width and length of the nacelle. In the red sector, the width of the cylinder for all visible wind turbines is set to the width of the blade, see Figure 2.5.

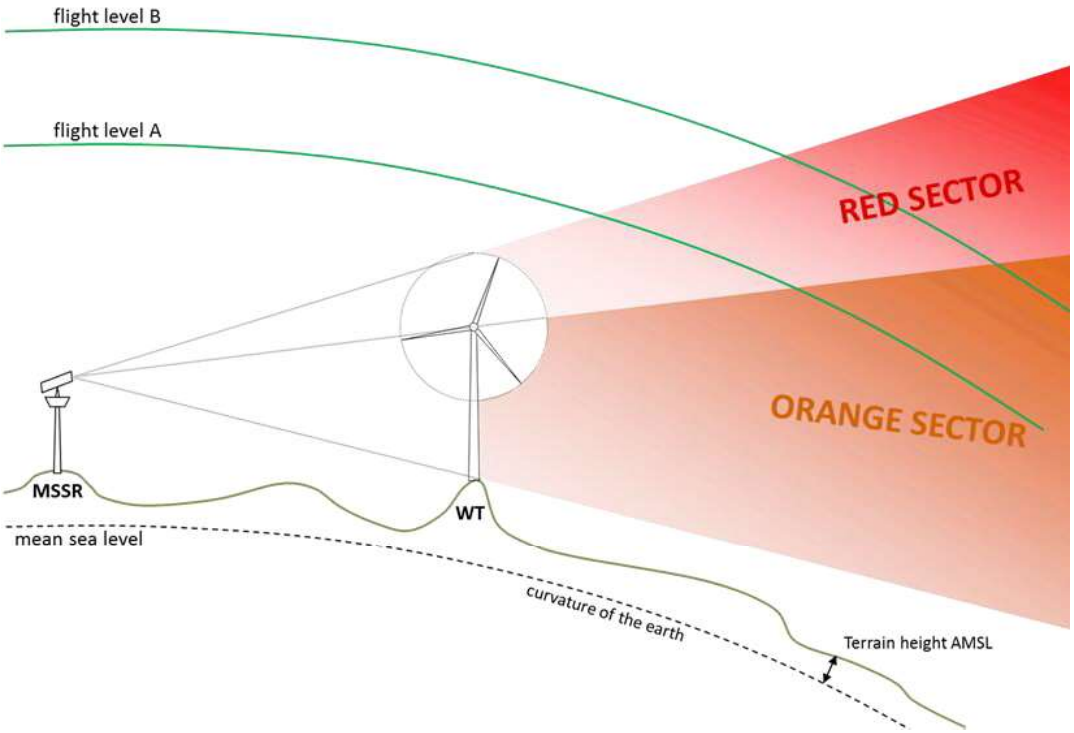

Figure 2.5 The orange and red areas, shown in the LoS coverage diagrams are in fact cuts through a volume behind the wind turbines. The calculated OBE (Off Boresight Error) is thus valid at all flight levels shown in the LoS coverage diagrams.

It is assumed that there is always a wind turbine blade with a vertical orientation. The full tip height of the turbine is used in the analysis. As there is not always a wind blade directed vertically, this is a worst-case assumption.

Furthermore, the applied method describes the incoming signal as a plane wave (as depicted in the left image of Figure 2.3). The approximation of the incoming radiation as a plane wave is valid in case the distance between the target and the obstacle is sufficiently large. To see whether the plane wave approximation is valid, we calculate at which distance the phase difference between the two ends of the wind turbine blade is equal to half a wavelength. The path difference Δr from one end of the blade to the other can be approximated by $\Delta r = L^2/2R$, where L is the length of the blade and R is the range. Setting Δr equal to half a wavelength, $\lambda/2$, and filling in for this example $L = 60.7$ meter, we find $R = 13$ km at 1090 MHz. We see that the incoming wave for a target at 13 km behind the obstacle already resembles a plane wave quite closely. For targets at larger distances the resemblance will be even better. For targets closer than 13 km to behind the wind turbine, the estimated bearing error is a first order approximation.

Regarding the geometry of the situation, we take into account two parameters: (1) the azimuth angle to the target, relative to the obstacle and (2) the orientation of the radar antenna at the moment that the transponder reply is received. Given a wind turbine at a certain azimuth angle, α, we let the target move from $\alpha - 4°$ to $\alpha + 4°$ in 501 steps. At more than 4° azimuth from the wind turbine the error reduces rapidly to values much smaller than the accuracy of the MSSR (typically 0.05°). For each position of the target, the radar antenna is rotated over 3°, from -1.5° to 1.5°, where 0° corresponds to the antenna looking directly at the target. For each geometry the disturbed electric field is calculated. This is done for each

(visible) wind turbine in the wind farm separately. Subsequently, all disturbed fields are summed and the bearing error for the total field is calculated.

A typical example of the Off-Boresight Error (OBE) for a single obstacle (i.e., cylinder width 25 meter) at a range of 3 km is shown in Figure 2.6. The obstacle is located at an azimuth angle of 218.5°. At a given azimuth angle, the error is in 100% of the cases contained within the two grey lines, in 90% of the cases between the two orange lines. The OBE at a given azimuth angle is thus not a single number, but lies in the range defined by the two lines of the same colour. The reason this happens, is that, as mentioned above, the geometry between the rotating antenna, target and obstacle can differ for a target at a given azimuth. The grey line thus gives the upper limit of the bearing error to be expected at a given azimuth angle. This is the case when the radar antenna is in the least favourable orientation when receiving the reply signal.

As can be seen in the figure below the OBE caused by a single obstacle is point symmetrical around the azimuth to the obstacle. Directly behind the obstacle, the error is zero. In this case the sum and difference beams are equally disturbed, resulting in no error of the estimated azimuth angle. Note that in the case of multiple obstacles at different ranges, the symmetry is broken.

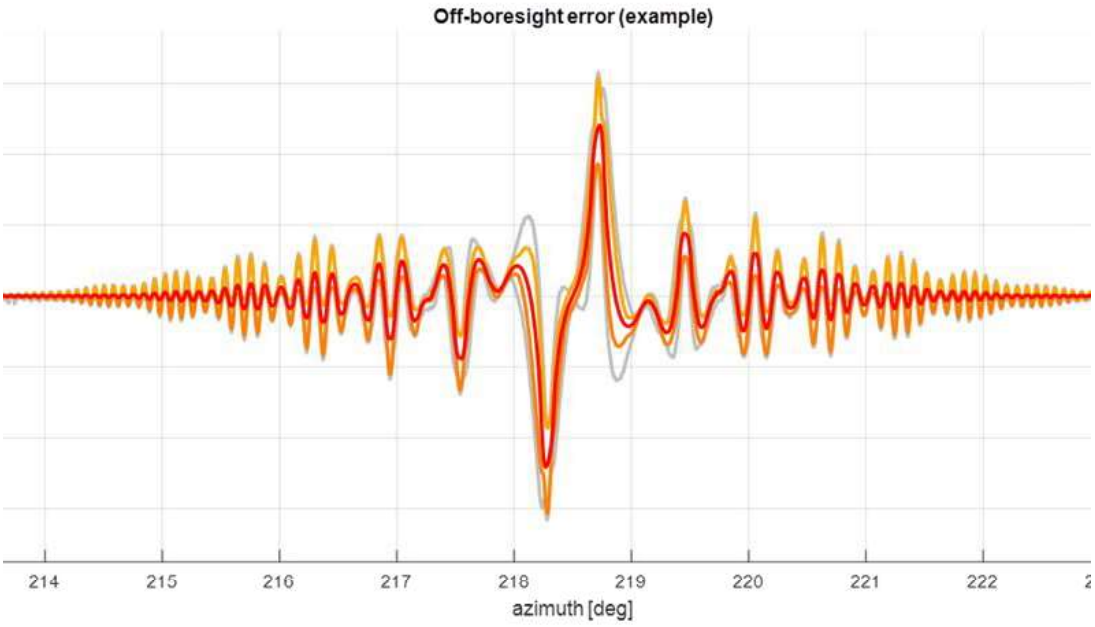

Figure 2.6 The off-boresight error for an infinite cylinder with a width of 25 m at a range of 3 km from the radar antenna. The error is point symmetrical around the azimuth angle to the obstacle.

3 Specific Input Parameters

3.1 Wind turbines

A DEA has been carried out for the newly planned wind turbines of Ballycar windfarm comprising twelve wind turbines. All already consented wind turbines near the newly planned wind turbines are also taken into account. An overview of the situation is provided in Figure 3.1. The red dots indicate the wind turbines under investigation and the cyan dots are the already consented wind turbines near the newly planned windfarm. The distance between the secondary radar at Woodcock Hill and the closest wind turbine of the newly planned windfarm measures approximately 2.5 km.

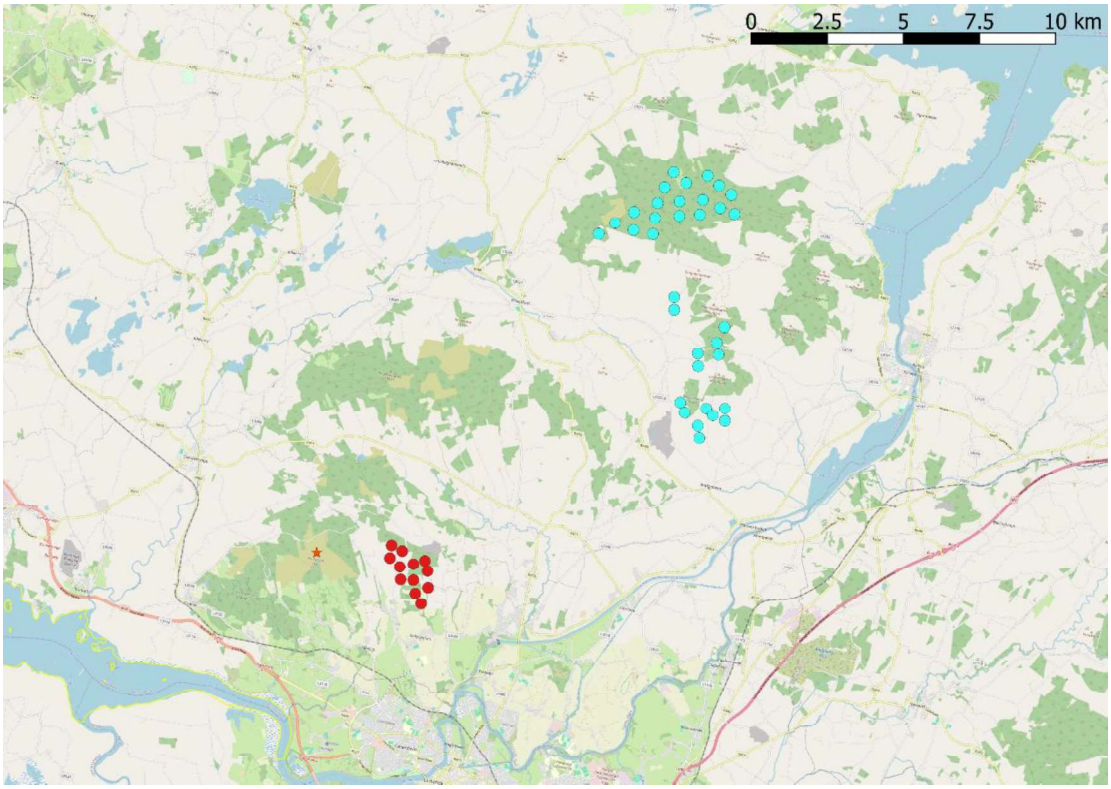

Figure 3.1 The locations of the newly planned windfarm Ballycar (red dots). The cyan dots correspond to the consented wind turbines near the newly planned wind turbines that are considered in this study. The secondary radar at Woodcock Hill is indicated by the red star. Image taken from OpenStreetMap.

In Table 3.1 an overview is presented of the positions, types, hub and tip heights of the already consented wind turbines near the newly planned wind turbines. The positions, type of the wind turbines and tip height have been received from Ai Bridges.

Table 3.1 Overview of the WGS84 longitude, latitude positions, type and tip heights of the already consented wind turbines near the newly planned wind turbines which have been provide by Ai Bridges. The UTM 29 N coordinates have been derived from these.

Nr.	Name/Owner	ID	UTM29N East [m]	UTM29N North [m]	Lat [°]	Lon [°]	Terrain [m]	Type	Hub [m]	Tip [m]
1	Carrownagowan WF	Car-01	526768	5853389	52.82960	-8.60269	247	N133 4.8MW	101	167.5
2	Carrownagowan WF	Car-02	527227	5853851	52.83373	-8.59585	255	N133 4.8MW	101	167.5
3	Carrownagowan WF	Car-03	527862	5853738	52.83268	-8.58642	305	N133 4.8MW	101	167.5
4	Carrownagowan WF	Car-04	528515	5853736	52.83263	-8.57673	333	N133 4.8MW	101	167.5
5	Carrownagowan WF	Car-05	527764	5854322	52.83794	-8.58783	252	N133 4.8MW	101	167.5
6	Carrownagowan WF	Car-06	528480	5854275	52.83748	-8.57721	259	N133 4.8MW	101	167.5
7	Carrownagowan WF	Car-07	529249	5854498	52.83944	-8.56578	253	N133 4.8MW	101	167.5
8	Carrownagowan WF	Car-08	529898	5854673	52.84098	-8.55612	324	N133 4.8MW	101	167.5
9	Carrownagowan WF	Car-09	528462	5854766	52.84189	-8.57743	237	N133 4.8MW	101	167.5
10	Carrownagowan WF	Car-10	529161	5854962	52.84362	-8.56704	243	N133 4.8MW	101	167.5
11	Carrownagowan WF	Car-11	529897	5855166	52.84541	-8.55609	284	N133 4.8MW	101	167.5
12	Carrownagowan WF	Car-12	530509	5855012	52.84399	-8.54702	317	N133 4.8MW	101	167.5
13	Carrownagowan WF	Car-13	531012	5854915	52.84309	-8.53957	321	N133 4.8MW	101	167.5
14	Carrownagowan WF	Car-14	530784	5855511	52.84846	-8.54289	317	N133 4.8MW	101	167.5
15	Carrownagowan WF	Car-15	530333	5855722	52.85038	-8.54958	286	N133 4.8MW	101	167.5
16	Carrownagowan WF	Car-16	529903	5855961	52.85255	-8.55593	251	N133 4.8MW	101	167.5
17	Carrownagowan WF	Car-17	529256	5855590	52.84925	-8.56558	222	N133 4.8MW	101	167.5
18	Carrownagowan WF	Car-18	528590	5855311	52.84679	-8.57548	208	N133 4.8MW	101	167.5
19	Carrownagowan WF	Car-19	528784	5855853	52.85165	-8.57256	189	N133 4.8MW	101	167.5
20	Fahy Beg	FaB-01	530492	5848480	52.78527	-8.54788	118	N133 4.8MW	110	176.5

Nr.	Name/Owner	ID	UTM29N East [m]	UTM29N North [m]	Lat [°]	Lon [°]	Terrain [m]	Type	Hub [m]	Tip [m]
21	Fahy Beg	FaB-02	530702	5848181	52.78257	-8.54479	142	N133 4.8MW	110	176.5
22	Fahy Beg	FaB-03	531368	5848452	52.78497	-8.53490	213	N133 4.8MW	110	176.5
23	Fahy Beg	FaB-04	531213	5847838	52.77946	-8.53725	151	N133 4.8MW	110	176.5
24	Fahy Beg	FaB-05	531338	5847457	52.77603	-8.53543	124	N133 4.8MW	110	176.5
25	Fahy Beg	FaB-06	531627	5848272	52.78333	-8.53108	185	N133 4.8MW	110	176.5
26	Fahy Beg	FaB-07	531974	5848575	52.78604	-8.52590	194	N133 4.8MW	110	176.5
27	Fahy Beg	FaB-08	532052	5848173	52.78242	-8.52478	154	N133 4.8MW	110	176.5
28	Lackareagh Wind Farm	Lac-01	529612	5851842	52.81555	-8.56063	225	V150 6MW	105	180
29	Lackareagh Wind Farm	Lac-02	529693	5851443	52.81196	-8.55946	183	V150 6MW	105	180
30	Lackareagh Wind Farm	Lac-03	531429	5851185	52.80953	-8.53374	364	V150 6MW	105	180
31	Lackareagh Wind Farm	Lac-04	531286	5850631	52.80456	-8.53590	287	V150 6MW	105	180
32	Lackareagh Wind Farm	Lac-05	531416	5850253	52.80116	-8.53401	305	V150 6MW	105	180
33	Lackareagh Wind Farm	Lac-06	530743	5850160	52.80036	-8.54401	203	V150 6MW	105	180
34	Lackareagh Wind Farm	Lac-07	530835	5849753	52.79670	-8.54267	204	V150 6MW	105	180

For the DEA of the secondary radar the dimensions of the mast, nacelle and turbine blades need to be known. The dimensions used within the simulations of the newly planned turbines have been derived from 3D CAD drawings of the turbines that are available in the TNO wind turbine dimension database. The length of the nacelle is defined as the distance from the ‘hub’ to the back of the nacelle. The width of the nacelle has been derived from the effective surface area of the front of the nacelle and could deviate slightly from the actual dimensions. The widths of the blades have been derived from the frontal area of the blade. The dimensions of the existing and authorised wind turbines are presented in Table 3.2.

.

Table 3.2 The dimensions of the consented wind turbines in the 20 km neighbourhood.

Wind Turbine Type	Manufacturer	Mast Length [m]	Mast ø top [m]	Mast ø base [m]	Nacelle Height [m]	Nacelle Width [m]	Nacelle Length [m]	Blade Length [m]	Blade Width [m]
N133@167.5	Nordex	98.9	3.3	4.3	4.7	5.1	16.3	66.5	3.7
N133@176.5	Nordex	107.9	3.3	4.3	4.7	5.1	16.3	66.5	3.7
V150EnVentus@180	Vestas	101.9	4.0	4.2	5.5	8.6	21.6	74.6	3.4

The position and dimensions of all newly planned wind turbines are presented in Figure 3.2 and in Table 3.3. The coordinates of the wind turbines are given in WGS84 coordinates and have been received from Ai Bridges. The UTM 29N coordinates have been derived from the WGS84 coordinates. The height of the ground level at the locations is given with respect to the EGM96 geoid and has been derived from the SRTM1 terrain height database.

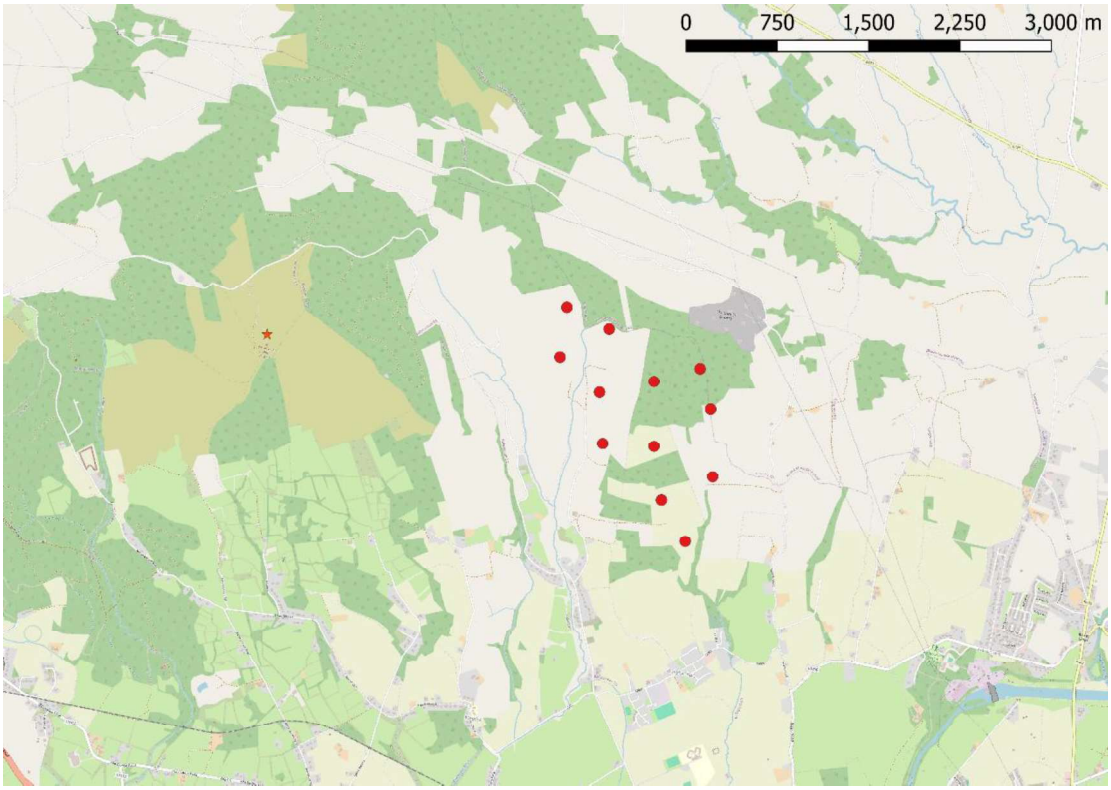

Figure 3.2 The twelve newly planned wind turbines of Ballycar windfarm (red dots) under investigation. Image taken using OpenStreetMap.

Table 3.3 Overview of the positions and tip heights newly planned wind turbines of Ballycar windfarm. The WGS84 Latitude and longitude coordinates and tip heights have been provided by Ai Bridges. The UTM 29N coordinates has been derived from these.

Location	ID	UTM29 N East [m]	UTM29 N North [m]	Lat [°]	Lon [°]	Terrain [m]	Tip Height AGL [m]
Ballycar	Bal-01	522132	5841989	52.72732	-8.67228	160	158
	Bal-02	522157	5841575	52.72360	-8.67193	162	158
	Bal-03	522508	5841879	52.72632	-8.66672	112	158

Location	ID	UTM29 N East [m]	UTM29 N North [m]	Lat [°]	Lon [°]	Terrain [m]	Tip Height AGL [m]
	Bal-04	522532	5841357	52.72163	-8.66639	106	158
	Bal-05	522954	5841532	52.72319	-8.66014	75	158
	Bal-06	523303	5841711	52.72478	-8.65495	265	158
	Bal-07	523455	5841403	52.72200	-8.65273	241	158
	Bal-08	523059	5841012	52.71850	-8.65862	265	158
	Bal-09	522641	5840951	52.71797	-8.66481	219	158
	Bal-10	523581	5840859	52.71711	-8.65090	192	158
	Bal-11	523207	5840589	52.71469	-8.65646	176	158
	Bal-12	523465	5840295	52.71205	-8.65266	176	158

The dimensions of the newly planned Ballycar wind turbines are based on the Vestas V136 with an output power of 4.5 MW and a hub height of 90 m, resulting in a tip height of 158 m. The dimensions of this wind turbine used within the simulations are listed in Table 3.4.

Table 3.4 The dimension of the newly planned wind turbines of Ballycar windfarm used within the simulations.

Wind Turbine Type	Manufacturer	Mast Length [m]	Mast ø top [m]	Mast ø base [m]	Nacelle Height [m]	Nacelle Width [m]	Nacelle Length [m]	Blade Length [m]	Blade Width [m]
V136@158	Vestas	87.8	3.3	3.9	4.8	4.8	17.6	67.7	3.1

3.2 Secondary Radar Woodcock Hill

The radar at Woodcock Hill is an en-route stand-alone MSSR, see Figure 3.3. The main parameters, coordinates and antenna height have been received from Ai Bridges Limited [3]. The radar parameters that are relevant for this study are presented in Table 3.5.

Figure 3.3 The stand-alone en-route MSSR at Woodcock Hill housed in a radome (Image source: IAA).

Table 3.5 Relevant radar parameters of the stand-alone MSSR at Woodcock Hill [3].

Parameter	Value
Antenna position	Stand-alone
X (UTM29N)	519760 E
Y (UTM29N)	5841280 N
Latitude (WGS84)	52.721047° N
Longitude (WGS84)	8.707438889° W
Height (EGM96)	10 m AGL
	307.8 m AMSL
Number of elements	35 m
Antenna length	8.5 m
Frequency	1090 MHz
Maximum Instrumented Range	256 NM

4 DEA of the MSSR at Woodcock Hill

In this section we determine the effect the presence of wind turbines can have on the performance of the stand-alone MSSR at Woodcock Hill. In order to do this, we first carry out the so-called Line-of-Sight (LoS) analysis for the MSSR. This analysis will give insight into the visibility of the wind farm as seen from the MSSR's position. In addition to the LoS analysis we also calculate the off-boresight error (OBE) the wind farm causes on the bearing measurements of the secondary radar.

The situation concerns the presence of already consented wind turbines and the newly planned wind turbines at Ballycar. An overview of the considered wind turbines is provided by Figure 4.1, similar to Figure 3.1. For the MSSR study only the wind turbines that are located nearby the sector of ±2° around the newly planned wind turbines (red dotted lines) need to be considered. However, for a complete analysis on the effects of the newly planned wind turbines, all consented wind turbines indicated mentioned in Section 3.1 are taken into account.

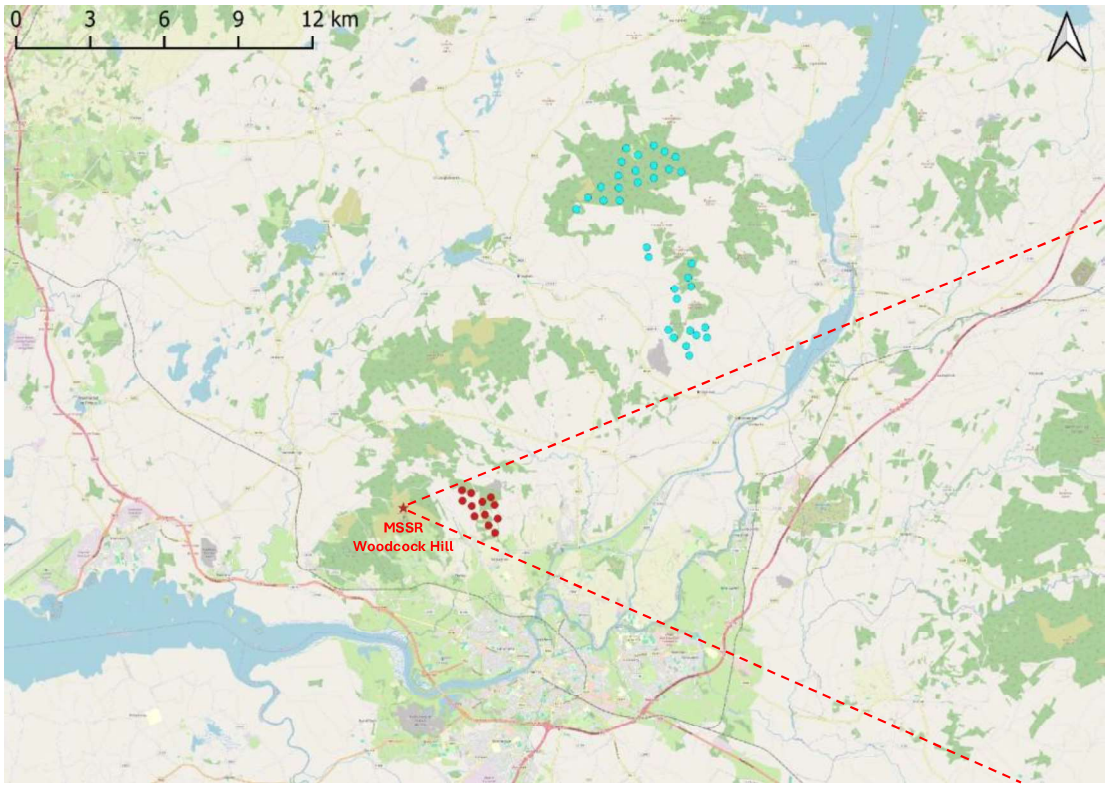

Figure 4.1 The locations of the newly planned windfarm Ballycar (red dots). The cyan dots correspond to the consented wind turbines near the newly planned wind turbines that are considered in this study. The secondary radar at Woodcock Hill is indicated by the red star. Image taken from OpenStreetMap.

In order to perform the Line-of-Sight analysis, a Digital Elevation Model (DEM) is required. The terrain altitude data in the DEM is taken from the Shuttle Radar Topography Mission (SRTM) database that has a resolution of approximately 25 meter. In Figure 4.2 an overview of the terrain altitude is shown. As can be observed, the terrain is a bit hilly. The radar location is shown, as well as the locations of the other consented and planned wind turbines.

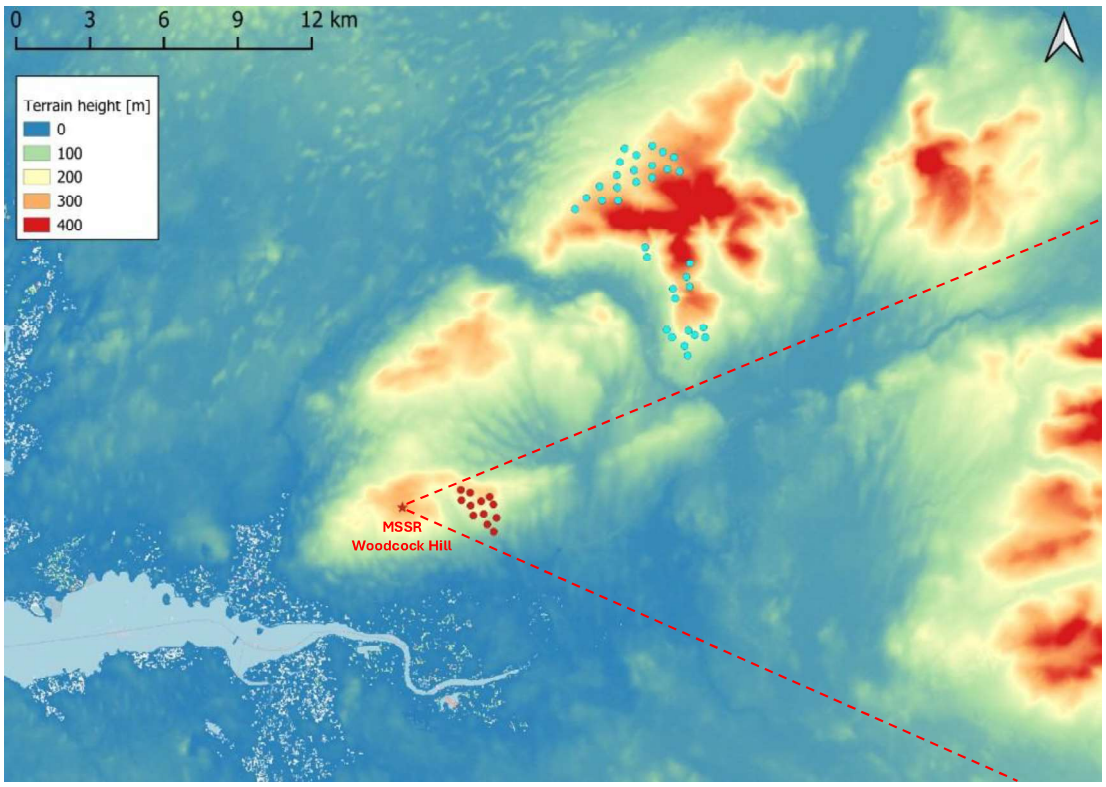

Figure 4.2 Height map around the newly planned wind turbines (red dots) showing the MSSR at Woodcock Hill (red star), and the consented wind turbines (cyan dots).

4.1 Radar horizon

In this section we show the extent of the wind farm in azimuth and elevation for the MSSR. These results reveal whether the wind farm has impact on the radar horizon. A wind turbine influences the radar horizon when the elevation angle to the tip height of the wind turbine is larger than the elevation angle to all other objects at the same azimuth angle, extending all the way up to the instrumented range of the MSSR, which measures 256 NM. Given the elevation angle to the tip height, aircraft at different altitudes are influenced at different ranges as shown in Figure 4.3. Here, the elevation angle to the tip height of the wind turbine is indicated by a grey line. The MSSR replies of aircraft above this line are not influenced by the wind turbine. Aircraft replies below the line may be influenced by the wind turbine.

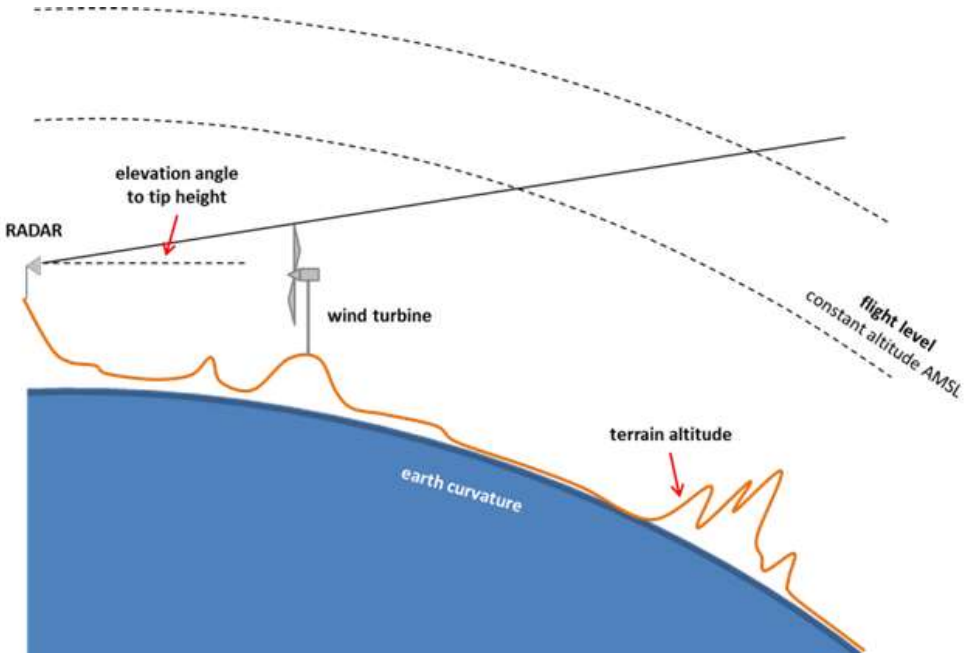

Figure 4.3 Overview of the overall Line-of-Sight geometry at fixed azimuth.

Note that this LoS analysis takes into account both the curvature of the Earth as well as the shape of the terrain. Electromagnetic waves do not follow straight lines, but tend to curve along the surface of the Earth to some extent as the refractivity index of the air varies with altitude. These refraction effects are generally taken into account by multiplying the radius of the Earth by a so-called *k*-factor. A common value for the *k*-factor is 1.33, which has been used in all results. By using the *k*-factor, we can treat the radio waves as if travelling along straight lines instead of curved lines.

In the next figure we show azimuth-elevation plots of the surrounding terrain (the radar horizon) including the wind farm. An orange (new) or green (existing and authorised) line indicates the wind turbine up to the tip height. The horizontal red lines indicate the blades of the wind turbine at hub height. Note that the scaling of the horizontal and vertical axes in these figures is different. This means that the wind turbines appear high and narrow. The width of the blades in the horizontal direction (azimuth) is in fact the actual width of the wind turbine as seen from the radar.

As can be seen in Figure 4.4 the radar has Line-of-Sight to the consented wind turbines as well as the newly planned wind turbines at Ballycar. The new turbines are planned at approximately 73° to 105° in azimuth with respect to the North as seen from the radar's location. As mentioned earlier, for the MSSR study only the wind turbines that are located nearby the sector of ±2° around the newly planned wind turbines need to be considered. Nevertheless, for completeness, all already existing wind turbines as shown in the figures below are taken into account.

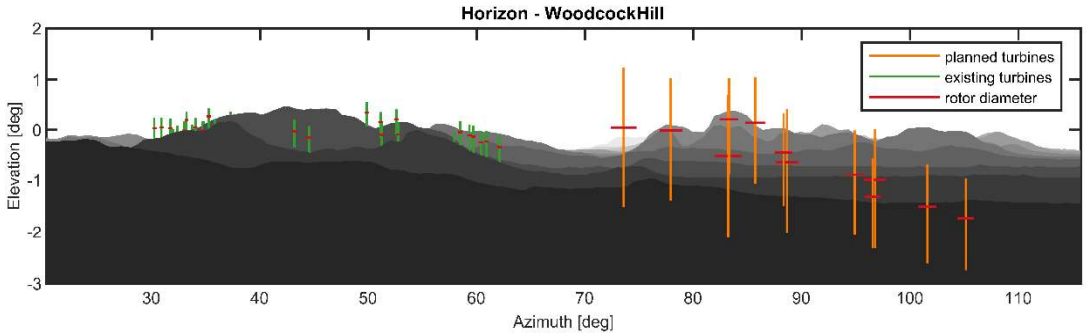

Figure 4.4 Horizon of the consented wind turbines as well as the newly planned wind turbines at Ballycar as seen from the MSSR.

4.2 Line-of-Sight to individual wind turbines

Next, we take a look at the Line-of-Sight to the individual wind turbines as seen from the MSSR. From these figures we can draw conclusions on aircraft ranges and altitudes at which the wind turbine potentially interferes with MSSR operations.

The red line in each figure represents 0 m AMSL. The black line above the red line shows the terrain altitude along the azimuth line towards the wind turbine. The radar is indicated by a red triangle on the left of each figure. The wind turbine is drawn at its corresponding range in each figure. The first Fresnel zone towards the tip and hub heights of the wind turbine are drawn as dashed red and blue ellipsoids, respectively.

A dashed black line passes through the point on the ground with the largest elevation angle as seen from the radar antenna. This is the point that determines the radar horizon in absence of the wind turbine. Furthermore, a red and orange zone are drawn. When orange and red zones are visible, the radar horizon is diminished by the wind turbine. The red zone indicates the reduction of the radar horizon due to the blades of the wind turbine. The orange zone indicates the reduction of the radar horizon by the mast of the wind turbine. In each figure, flight levels at 5000 ft, 7000 ft and 10000 ft are shown as well.

Note that in the red and orange areas the radar is not completely ‘blind’. The red and orange colours merely indicate where impact of the wind turbines on the radar performance can potentially occur. In these regions the signal from a transponder towards the SSR antenna passes a wind turbine. This means that the wave front of the signal transmitted by the transponder will be disturbed by the wind turbine and does not necessarily mean that the impact on the position estimation of the target by the MSSR is significant. The error in the position estimation due to wind turbines placed in the signal path is further investigated in Section 4.4.

Figure 4.5 and Figure 4.6 show the Line-of-Sight as seen from the MSSR towards a newly planned wind turbine at Ballycar. As can be seen, the radar has Line-of-Sight towards the wind turbine. At a range of 100 km, at the azimuth angle towards the wind turbine, a target below approx. 12390 ft might be obscured by the wind turbine (red and orange zones) and above that altitude the radar looks over the tip height of the turbine and the signal will not be obscured. For a target below approximately 2762 ft the radar signal will be behind the hills or horizon anyway.

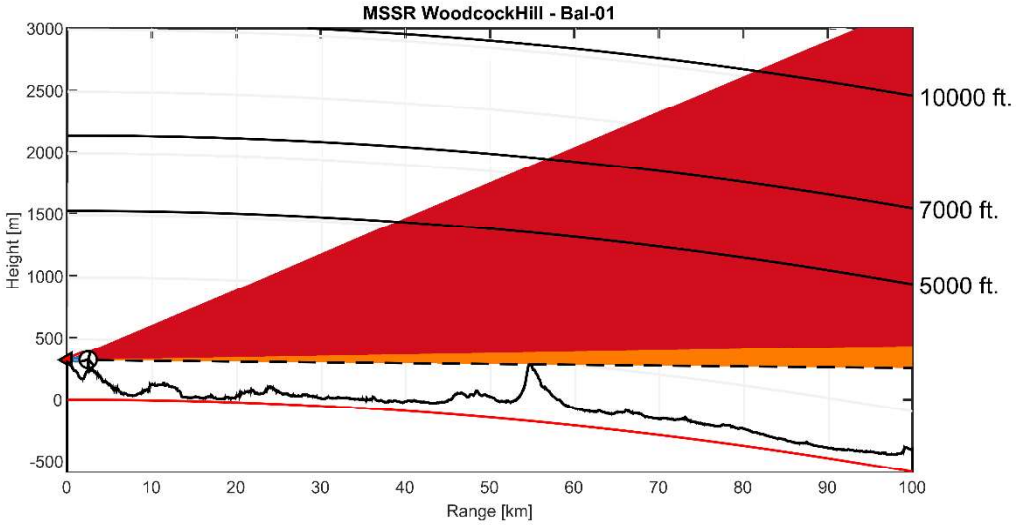

Figure 4.5 Line-of-Sight towards planned turbine Bal-01 as seen from the MSSR.

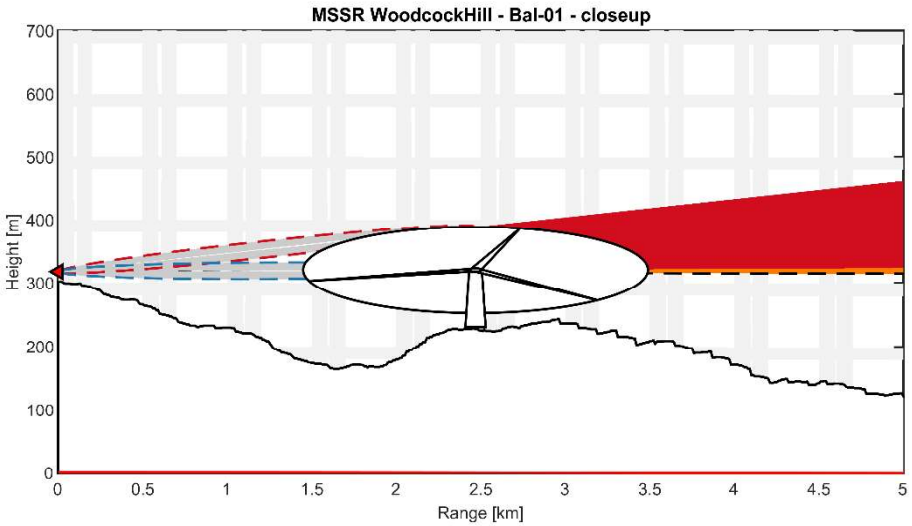

Figure 4.6 Closeup of Line-of-Sight towards planned turbine Bal-01 as seen from the MSSR.

It can be seen that the presence of the red area is significant, while the presence of the orange area is minimal, which is due to the close distance of the wind turbine to the radar. For most of the other newly planned wind turbines at Ballycar, the results are similar. However, some of these wind turbines are located in between the radar system and a hill that (mostly) obscures the Line-of-Sight of an aircraft at certain altitudes. In these cases, of which an example (Bal-10) is shown in Figure 4.7 and Figure 4.8, the aircraft is either behind this hill (i.e., below the dotted line) or is in direct Line-of-Sight of the radar without potential interference of the planned wind turbine (i.e., above the dotted line). Here, at a range of 100 km, at the azimuth angle towards the wind turbine, a target below approximately 2419 ft the radar signal will be behind the hills, and above this will not be affected by the wind turbine.

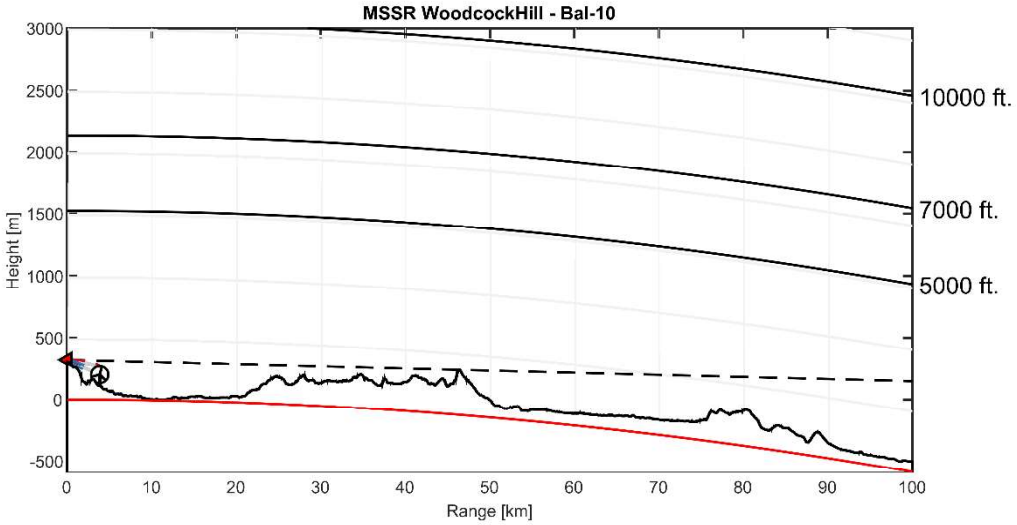

Figure 4.7 Line-of-Sight towards planned turbine Bal-10 as seen from the MSSR.

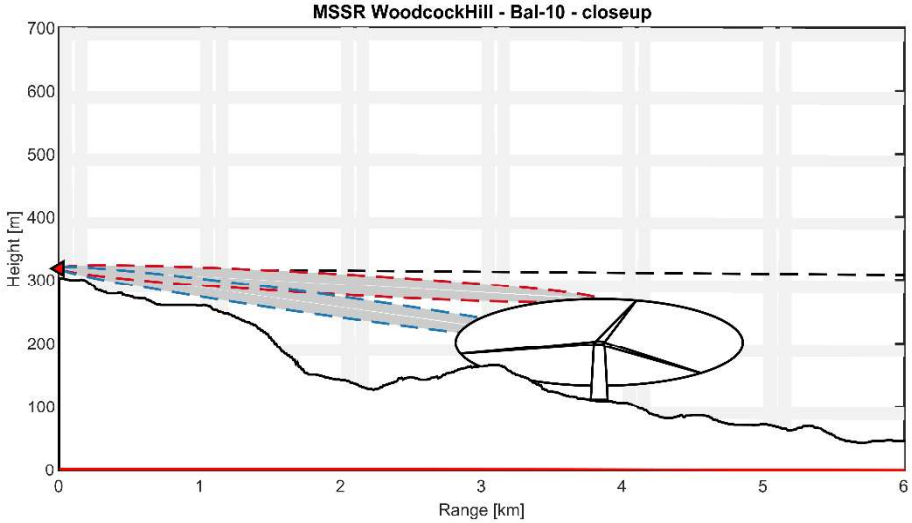

Figure 4.8 Closeup of Line-of-Sight towards planned turbine Bal-10 as seen from the MSSR.

Although not all consented wind turbines are within the sector of ±2° around the newly planned wind turbines as seen from the MSSR, for completeness, the results of the Line-of-Sight analysis to all wind turbines are summarized in the table below.

Table 4.1 Summary of heights at 100 km ground range where the wind turbine might influence the MSSR.

Nr.	Name	Unobscured Height [ft]	Obscured Height [ft]
1	Car-01	1868	4974
2	Car-02	2229	5044
3	Car-03	3105	6107
4	Car-04	4576	6622
5	Car-05	2723	4862
6	Car-06	3486	4953
7	Car-07	4902	4733

Nr.	Name	Unobscured Height [ft]	Obscured Height [ft]
8	Car-08	5619	6047
9	Car-09	3061	4439
10	Car-10	4094	4488
11	Car-11	5226	5197
12	Car-12	5918	5778
13	Car-13	5591	5805
14	Car-14	5756	5669
15	Car-15	5276	5119
16	Car-16	4209	4483
17	Car-17	3284	4014
18	Car-18	2938	3797
19	Car-19	2819	3385
20	FaB-01	4276	2132
21	FaB-02	3332	2742
22	FaB-03	3152	4439
23	FaB-04	3040	2961
24	FaB-05	2599	2288
25	FaB-06	3152	3752
26	FaB-07	3128	3918
27	FaB-08	2944	2999
28	Lac-01	6436	4679
29	Lac-02	6542	3745
30	Lac-03	3596	7536
31	Lac-04	3880	5992
32	Lac-05	4342	6427
33	Lac-06	3899	4219
34	Lac-07	4398	4265
35	Bal-01	2762	12390
36	Bal-02	6401	8404
37	Bal-03	3849	10898
38	Bal-04	3004	6266
39	Bal-05	3341	11047
40	Bal-06	6374	10851
41	Bal-07	3351	5680
42	Bal-08	2594	2930
43	Bal-09	2306	3168
44	Bal-10	2419	-1191
45	Bal-11	3436	-2129

Nr.	Name	Unobscured Height [ft]	Obscured Height [ft]
46	Bal-12	2566	-4377

As can be observed from the diagrams and tables above, there is full line of sight between the radar and all the consented and newly planned wind turbines.

4.3 Line-of-Sight coverage

The results in the previous sections give insight to which extent the wind farm can potentially affect the bearing estimate provided by the MSSR. In this section we show the locations of the affected areas in the Line-of-Sight coverage diagrams. Coverage diagrams are shown for targets at altitudes of 5000, 7000, 10000 and 35000 ft for the consented situation and after the newly planned wind turbines has been built. A coverage diagram shows whether the performance of the secondary radar can be influenced by the target at a given altitude.

The affected azimuth sector of a single wind turbine is taken as 5° on both sides of the wind turbine, 10° in total. As discussed in Section 2.1 in more detail, outside this 5° sector the impact of the wind turbine on the bearing determination will be smaller than the MSSR bearing accuracy.

The Line-of-Sight coverage diagrams for the MSSR at target heights of 5000, 7000, 10000 and 35000 ft are shown in the figures below. Areas affected by the mast up to the hub height of the wind turbines are shown in orange. Areas affected from hub height up to the tip height are shown in red. The radar is indicated by a red star, the yellow dots are the newly planned wind turbines and the blue dots are the consented wind turbines.

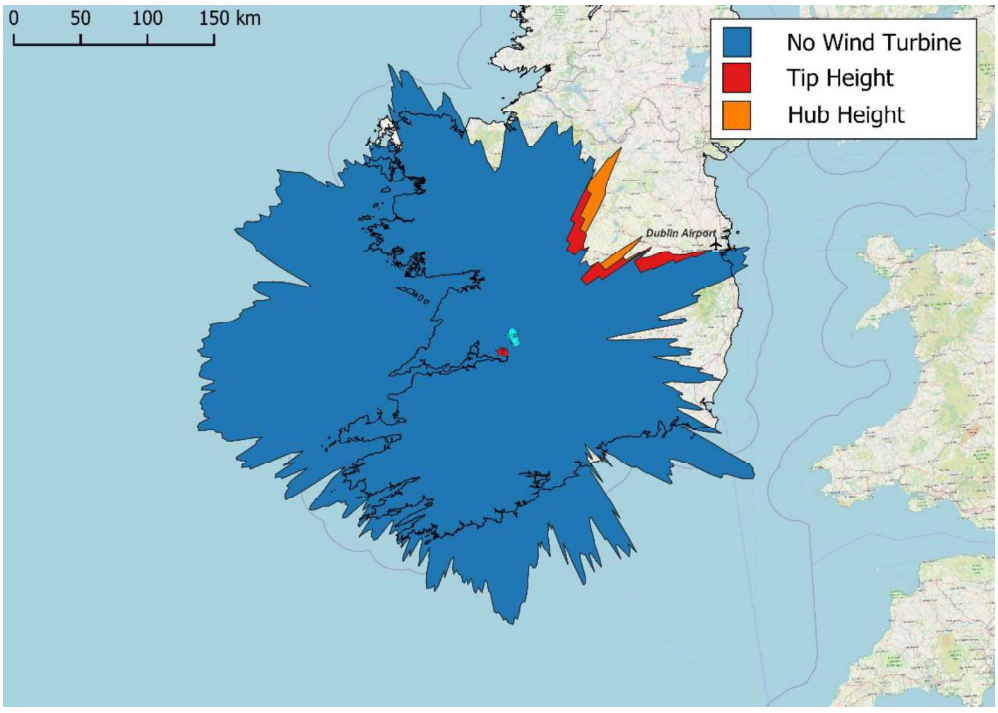

Figure 4.9 Line-of-Sight coverage diagram for a target at 5000 ft AMSL as seen from the MSSR. Only the consented wind turbines are taken into account.

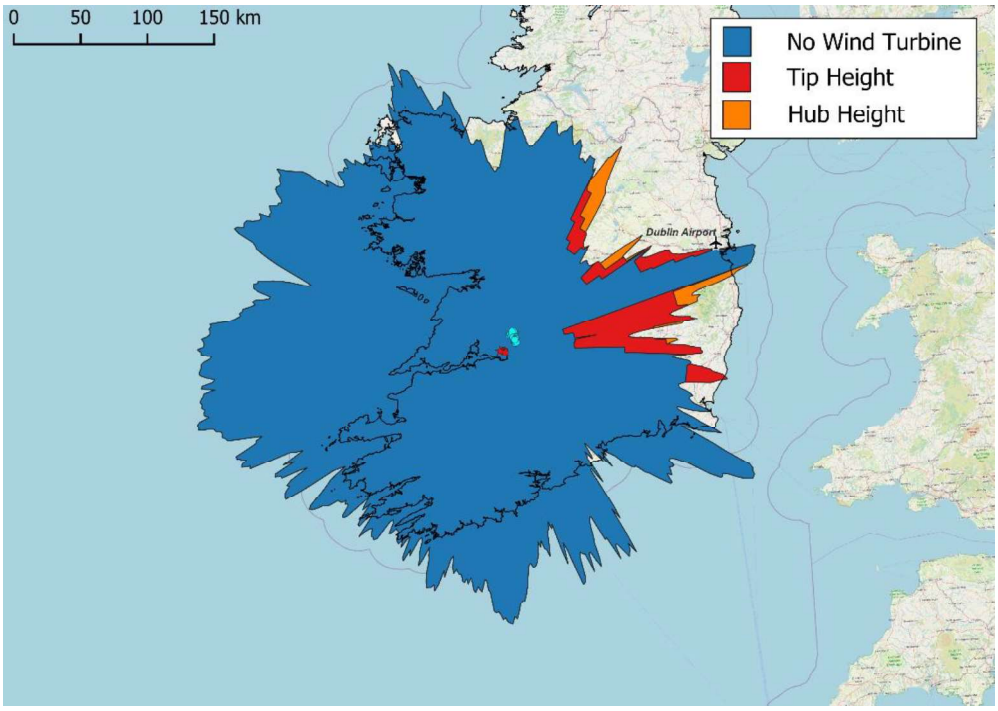

Figure 4.10 Line-of-Sight coverage diagram for a target at 5000 ft AMSL as seen from the MSSR. All consented wind turbines, and the newly planned wind turbine at Ballycar are taken into account.

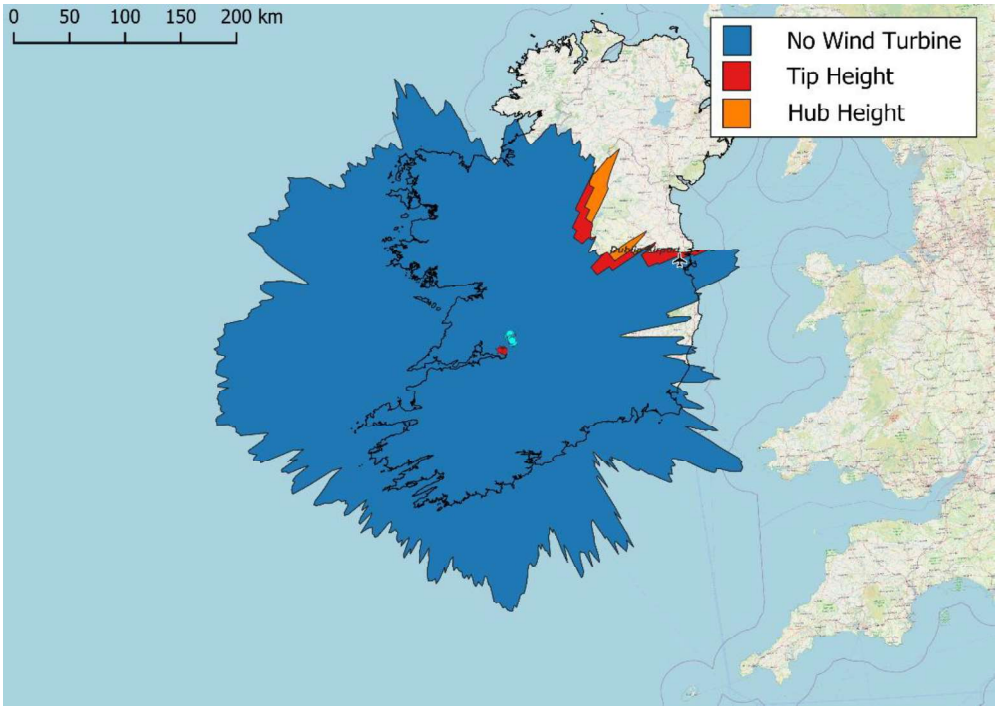

Figure 4.11 Line-of-Sight coverage diagram for a target at 7000 ft AMSL as seen from the MSSR. Only the consented wind turbines are taken into account.

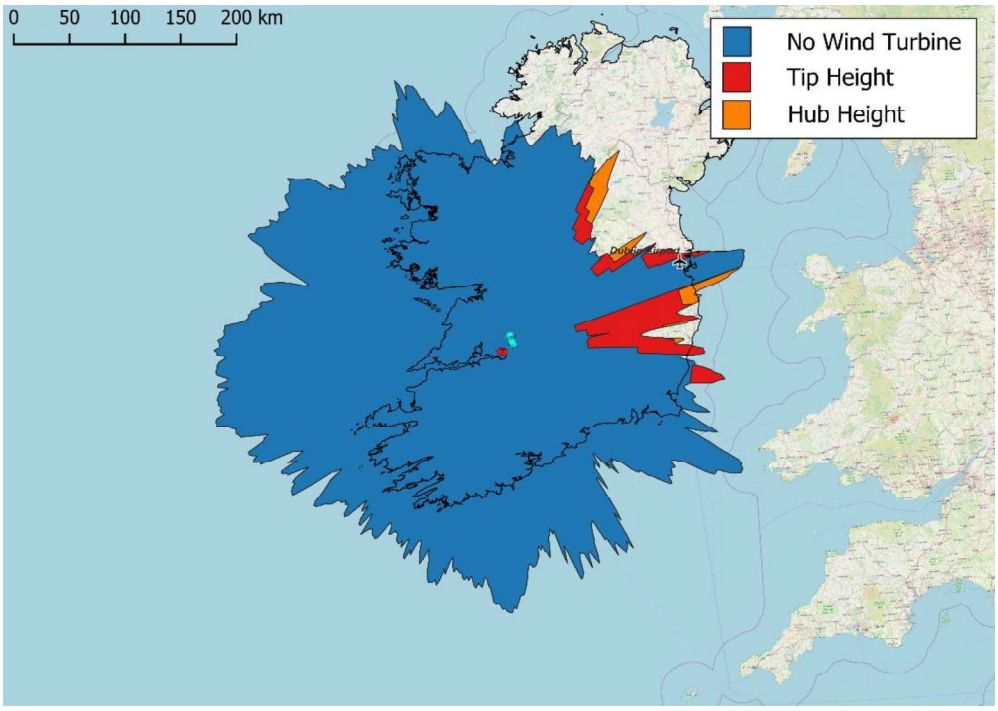

Figure 4.12 Line-of-Sight coverage diagram for a target at 7000 ft AMSL as seen from the MSSR. All consented wind turbines, and the newly planned wind turbine at Ballycar are taken into account.

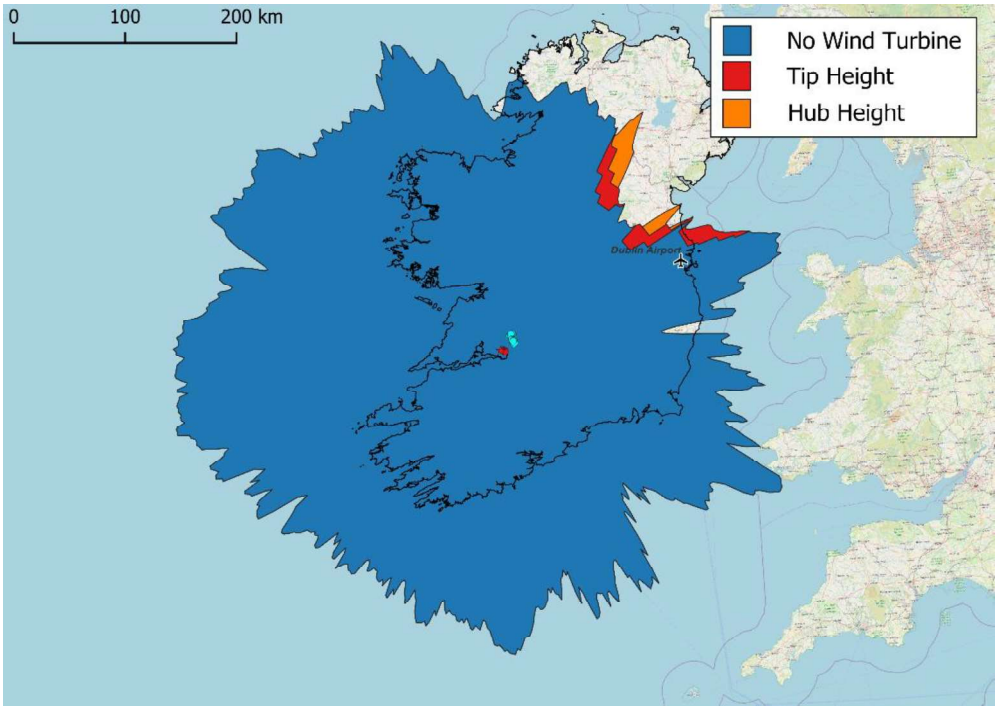

Figure 4.13 Line-of-Sight coverage diagram for a target at 10000 ft AMSL as seen from the MSSR. Only the consented wind turbines are taken into account.

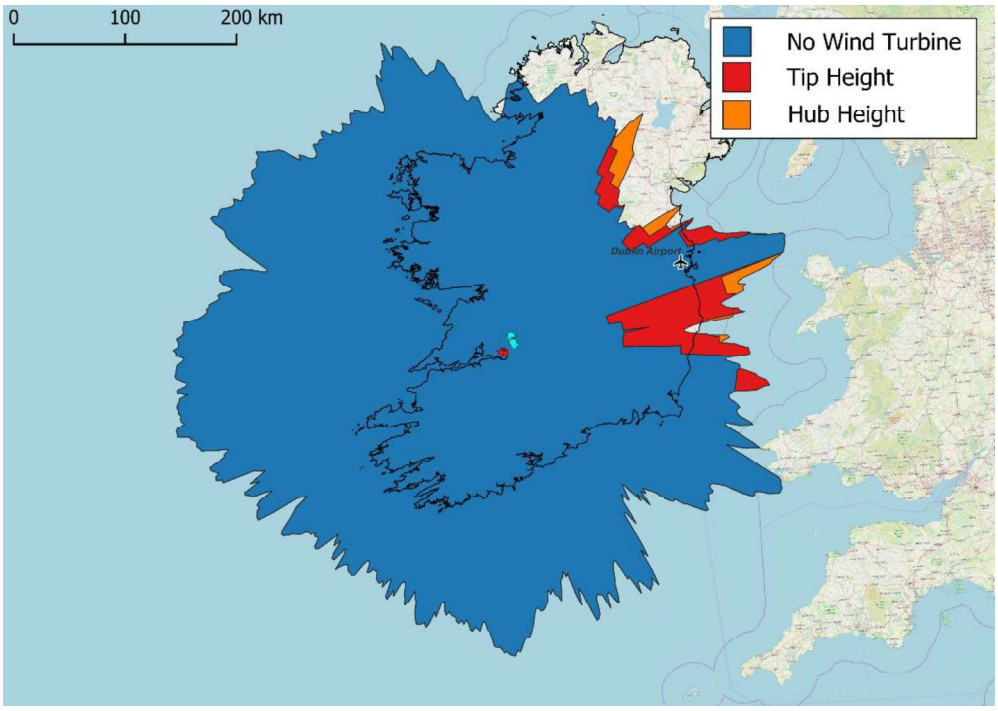

Figure 4.14 Line-of-Sight coverage diagram for a target at 10000 ft AMSL as seen from the MSSR. All consented wind turbines, and the newly planned wind turbine at Ballycar are taken into account.

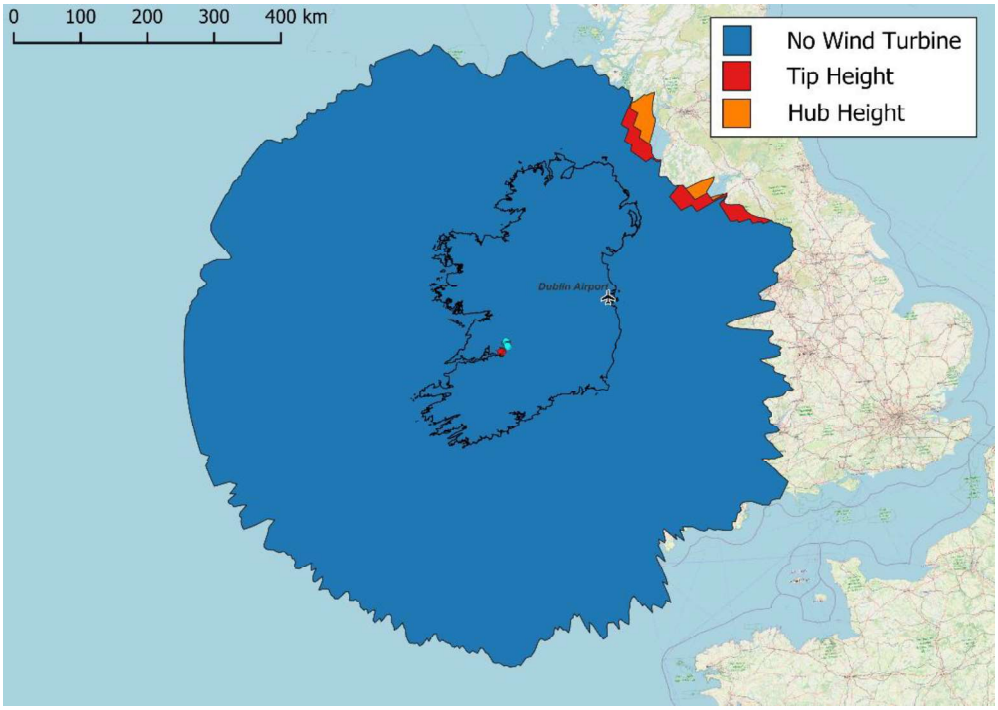

Figure 4.15 Line-of-Sight coverage diagram for a target at 35000 ft AMSL as seen from the MSSR. Only the consented wind turbines are taken into account.

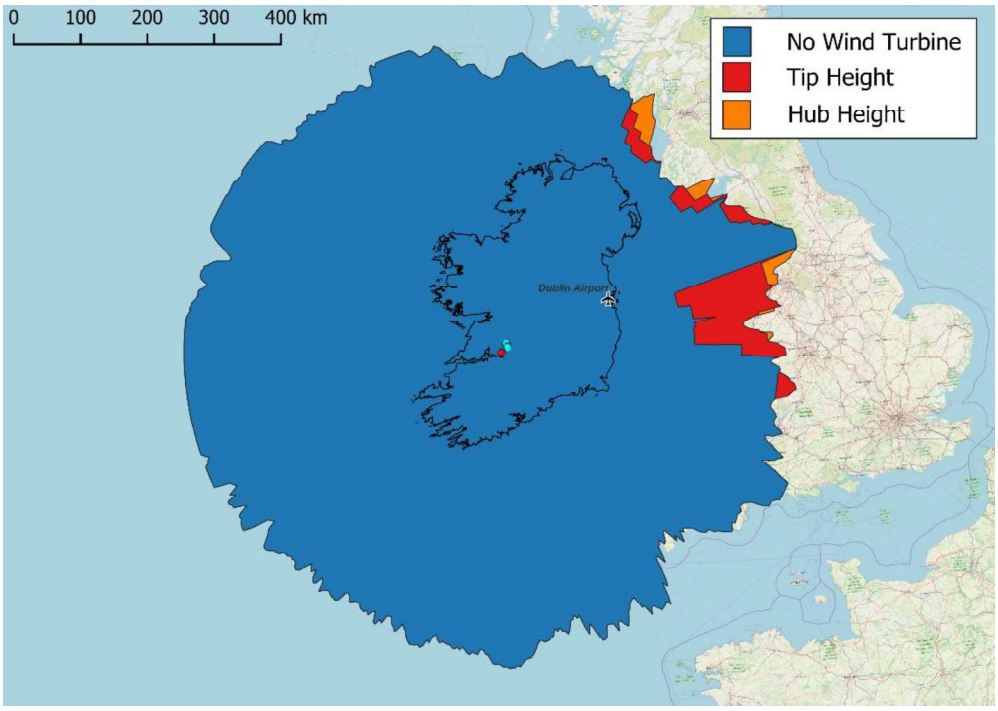

Figure 4.16 Line-of-Sight coverage diagram for a target at 35000 ft AMSL as seen from the MSSR. All consented wind turbines, and the newly planned wind turbine at Ballycar are taken into account.

In the figures it can be observed in the situation with the newly planned wind turbines at Ballycar result in a zone of additional coverage loss at an azimuth range of approximately 70° to 110° as seen from the radar.

4.4 Results of the OBE calculations

As stated in Section 2.1, the presence of an obstacle (like a mountain, building or wind turbine) between the MSSR antenna and the target can cause an error in the estimation of the bearing to the target. In this section, the extent of this bearing error is calculated using a model developed by TNO, in which the method described in Section 2.1 has been implemented.

In this section, the OBE calculations are presented for the MSSR. For the orange and red areas, shown in the figures in the previous section, OBE calculations were carried out. The OBE in the case of the planned wind turbines is determined. The OBE for each area is presented in two different figures for the planned wind turbines, resulting in a total of four figures.

Note that the OBE calculations are valid for all flight levels shown in the Line-of-Sight coverage diagrams in the previous section. We only need to do one calculation of the maximum azimuth errors per percentile for all red areas and one for all orange areas.

The results are plotted with a 100th-, a 90th-, and a 50th-percentile plot, in grey, yellow, and dark orange respectively. This is done to give a general overview of the distribution of the off-boresight error for a given azimuth angle. It also shows the same graphs, divided up into azimuth bins, with their values made absolute to create certain azimuth sectors, in which the maximum error can be analysed.

4.4.1 MSSR – Orange Area

In Figure 4.17, the OBE for the MSSR as a function of azimuth for the orange area in the previous results for the consented wind turbines is presented, similar to as in Section 2.1 (i.e., the area where the errors originate from the mast and the nacelle). As can be seen, the maximum absolute error is around 0.37° and the azimuth sector influenced by the consented wind turbines ranges from approximately 26° to 65° as seen from the MSSR. For the situation for the consented and newly planned wind turbines at Ballycar, this graph is shown in Figure 4.18. As can be seen, the maximum absolute error increases to 0.45° and the azimuth sector due to the newly planned wind turbines ranges from approximately 70° to 110° as seen from the MSSR.

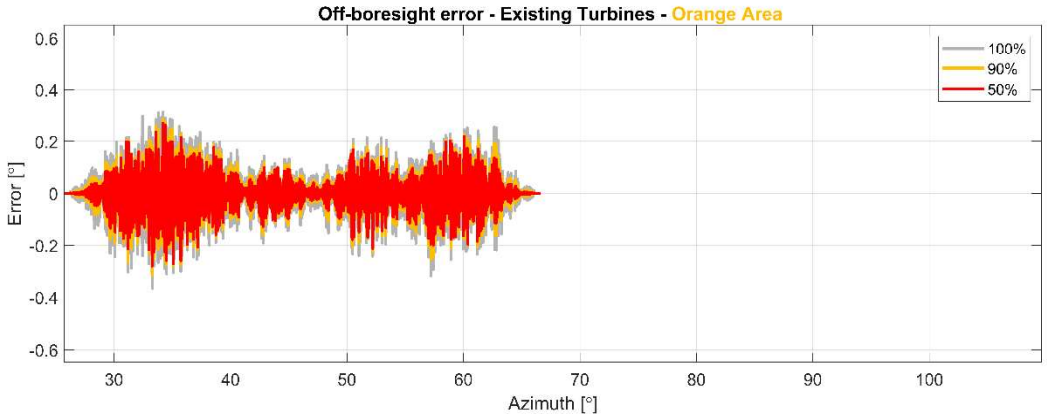

Figure 4.17 The off-boresight error for the consented wind turbines as a function of azimuth for the MSSR in the orange areas of the figures shown in Section 4.3 (i.e., the area where the errors originate from the mast and nacelle).

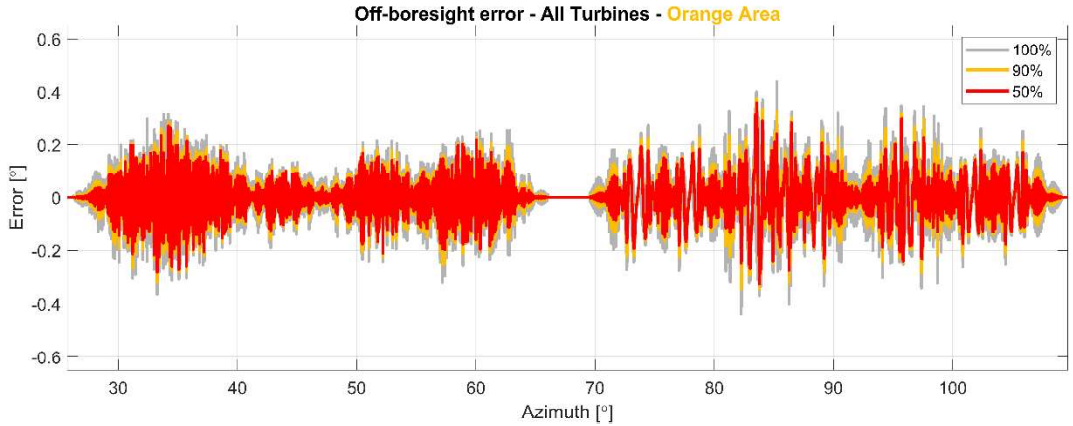

Figure 4.18 The off-boresight error for the consented and newly planned wind turbines at Ballycar as a function of azimuth for the MSSR in the orange areas of the figures shown in Section 4.3 (i.e., the area where the errors originate from the mast and nacelle).

As can be seen, the OBE fluctuates quite rapidly with azimuth angle. It therefore makes sense to look at the envelope of the graphs. Also, only the absolute value of the error is interesting. In Figure 4.19 we therefore present the same graphs for the situation with the consented wind turbines in a slightly different manner. In these figures, the absolute OBE is grouped per azimuth sector of 1°. For each azimuth sector the value of the 50th, 90th and 100th percentile are shown in red, orange and grey, respectively. The standard deviation, corresponding to a percentile of 68% assuming a normal distribution of the errors, of the OBE

is shown as a black dotted line. This distribution is also computed for the situation with the consented and newly planned wind turbines at Ballycar, as shown in Figure 4.20.

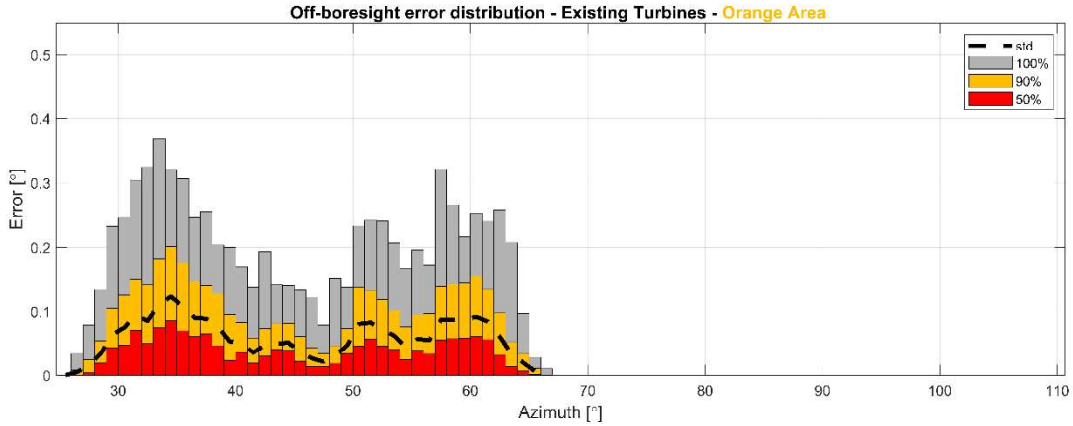

Figure 4.19 The cumulative distribution of the absolute OBE in the orange areas due to the consented wind turbines, per azimuth sector of 1.0°.

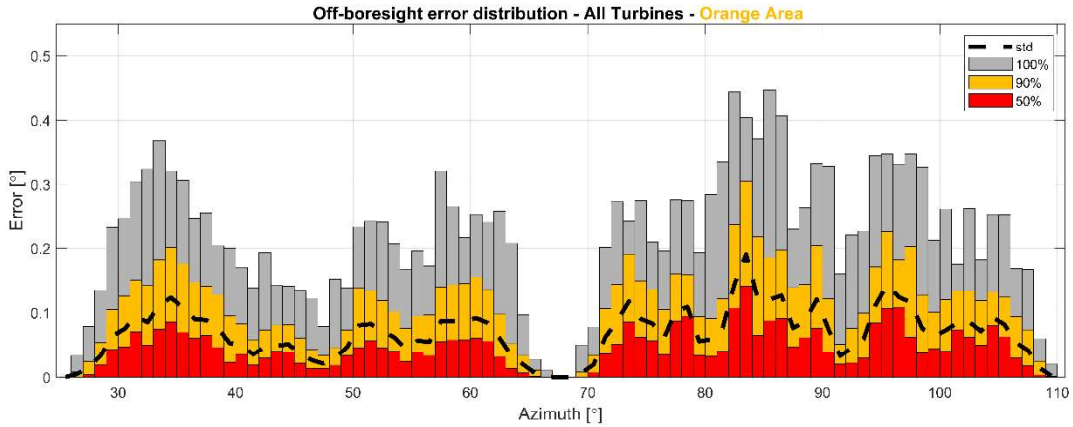

Figure 4.20 The cumulative distribution of the absolute OBE in the orange areas due to the consented and newly planned wind turbines at Ballycar, per azimuth sector of 1.0°.

In the first situation, the maximum OBE in the orange area occurs at an azimuth of approximately 33° at around 0.37°. This increases up to an OBE of 0.45°, which occurs around an azimuth of approximately 86°. However, as the 90th percentile indicates, in 90% of the cases, the maximum OBE is less than 0.20° in the initial situation, and increases up to 0.31° when the newly planned wind turbines at Ballycar are present. In 50% of the cases the maximum OBE is less than 0.10° in the initial situation and increases only to 0.14° in the new situation that includes the newly planned wind turbines at Ballycar.

4.4.2 MSSR – Red Area

In Figure 4.21, the OBE for the MSSR as a function of azimuth in the red area in the previous results for the consented wind turbines is presented (i.e., the area where the errors originate from the blade standing in the upright direction). In Figure 4.23 the absolute OBE is grouped per azimuth sector of 1° and the OBE distribution is shown. For the situation for both the consented and newly planned wind turbines at Ballycar the graph is shown in Figure 4.22 and Figure 4.24.

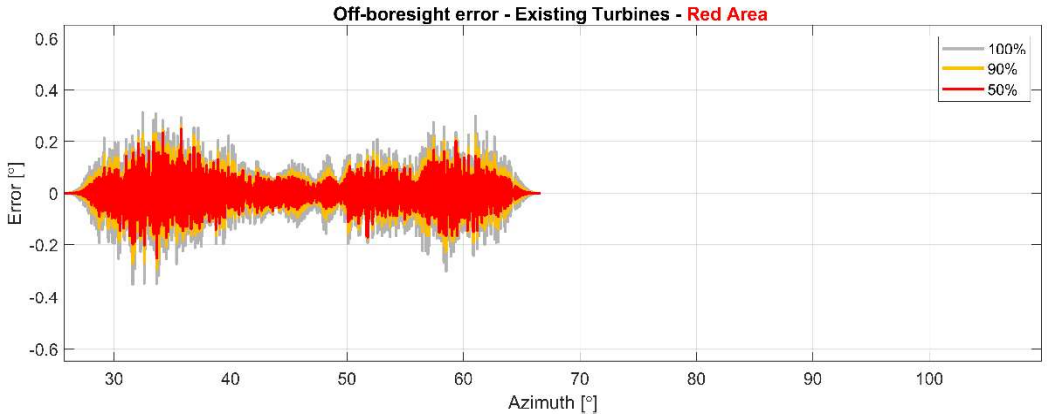

Figure 4.21 The off-boresight error for the consented wind turbines as a function of azimuth for the MSSR in the red areas of the figures shown in Section 4.3 (i.e., the area where the errors originate from the blades).

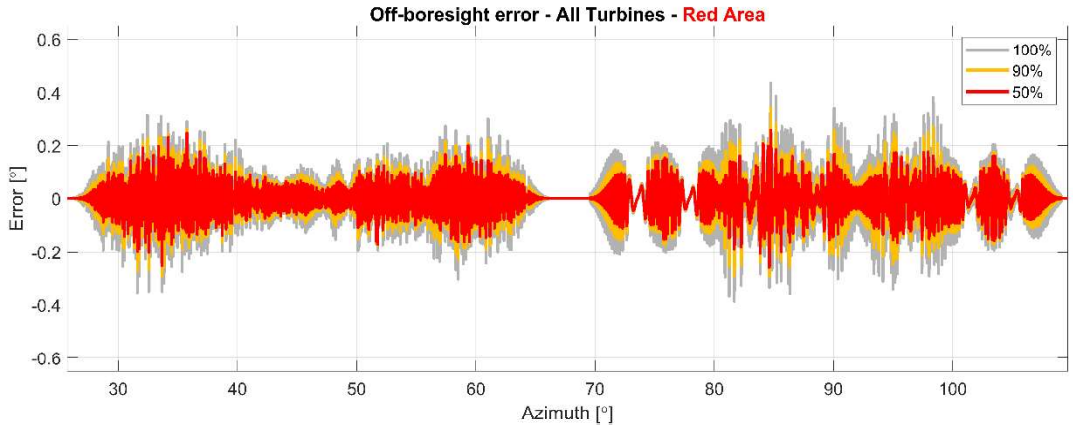

Figure 4.22 The off-boresight error for the consented and newly planned wind turbines at Ballycar as a function of azimuth for the MSSR in the red areas of the figures shown in Section 4.3 (i.e., the area where the errors originate from the blades).

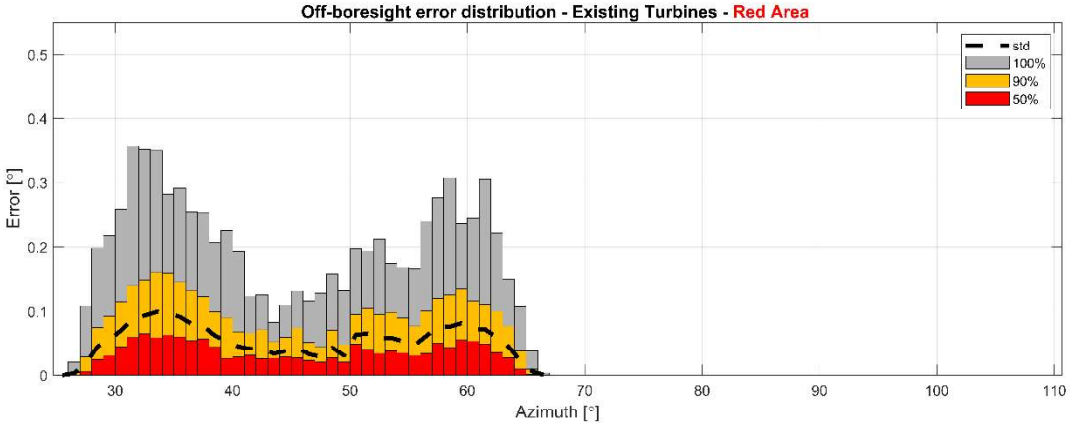

Figure 4.23 The cumulative distribution of the absolute OBE in the red areas due to the consented wind turbines, per azimuth sector of 1.0°.

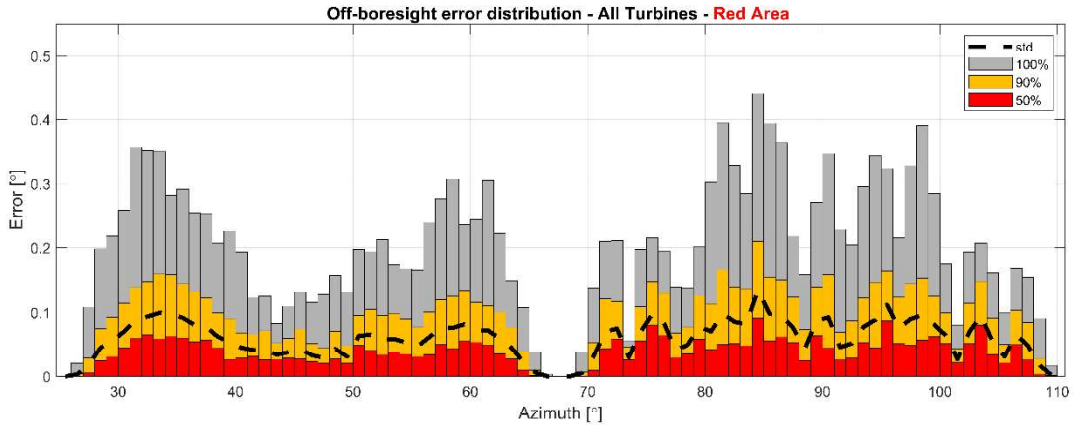

Figure 4.24 The cumulative distribution of the absolute OBE in the red areas due to the consented and newly planned wind turbines at Ballycar, per azimuth sector of 1.0°.

As can be seen in the OBE distribution graphs, the maximum absolute error in the red areas is 0.36° in the initial situation, and increases to 0.44° in the scenario with the wind turbines at Ballycar added. Moreover, as the 90th percentile indicates, in 90% of the cases the maximum OBE increases from 0.16° to 0.21° when the newly planned wind turbines at Ballycar are present. In 50% of the cases the maximum OBE is less than 0.09° for both situations.

4.4.3 Summary of OBE Results

The results of the previous sections are summarized in Table 4.2.This table shows the maximum 100th, 90th and 50th percentile errors, which are in degrees and describes the error off of true boresight azimuth of a target. The table also shows a standard deviation over the entire azimuth range. Besides, the “Orange Area” describes the situation where only the mast of the turbines is considered, and the “Red Area” describes the situation where both the mast and the rotor are considered.

Table 4.2 OBE statistics of the MSSR in the azimuth with the largest OBE error [°].

Scenario	100%	90%	50%	σ
Before new wind turbines, Orange	0.37	0.20	0.09	0.123
Before new wind turbines, Red	0.36	0.16	0.06	0.099
With new wind turbines at Ballycar, Orange	0.45	0.31	0.14	0.191
With new wind turbines at Ballycar, Red	0.44	0.21	0.09	0.134

As can be observed for the 100’th percentile and the 90’th percentile the maximum errors are higher after adding the newly planned wind turbines, and for the 50’th percentile the maximum expected errors are only slightly higher.

4.4.4 Interpretation of the results

As discussed, there exist many different geometries between the target, obstacle (wind turbine) and MSSR antenna. This means that the OBE can be different for two targets at the same azimuth at different moments. For each azimuth sector, the standard deviation is shown as well. For a normal distribution, the standard deviation corresponds to the 68th percentile. Here, the error data is not normally distributed. The standard deviation lies between the 50th and 90th percentile, nonetheless.

Comparing the affected azimuth sectors we see that the OBE extends up to approximately 4.5° to the left and to the right of the wind farm. Outside this 4.5° the OBE will not completely disappear, but it will be much smaller than the overall accuracy of the MSSR of 0.05° RMS. Outside the 4.5° the bearing error will therefore be dominated by other error sources than the wind farm. Note that in Section 4.3 a margin of 5° was assumed. Looking at the results of the OBE, this is indeed a reasonable assumption.

To put the errors in perspective, we can express the OBE in an error in cross-range at a certain distance. By cross-range, we mean the direction perpendicular to the viewing direction of the MSSR.

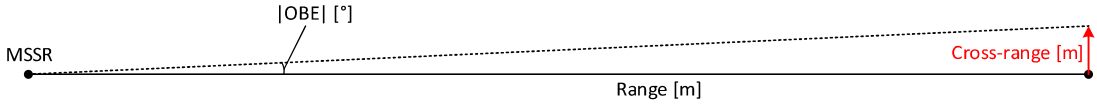

Figure 4.25 Projection of an OBE to a cross-range at a certain range (distance from the radar).

We have done this for the three values mentioned above, *i.e.*, 50, 90, and 100% percentile and for distances from the MSSR of 50, 100, 200, 222 and 278 km. The values are shown below in Table 4.3. As can be seen in the table, the 90th percentile OBE of 0.16° corresponds to a maximum cross-range error of 279 meter at a distance of 100 km.

Table 4.3 Example of bearing errors converted into cross-range error in meters for various distances from the MSSR.

		Cross-range error					
OBE	Percentile	Range to target					
[°]	[%]	50 km	100 km	200 km	222 km	278 km	474 km
		27 NM	54 NM	108 NM	120 NM	150 NM	256 NM
0.10	σ	87 m	175 m	349 m	387 m	485 m	827 m
0.06	50	52 m	105 m	209 m	232 m	291 m	496 m
0.16	90	140 m	279 m	559 m	620 m	776 m	1324 m
0.42	100	367 m	733 m	1466 m	1627 m	2038 m	3475 m

4.4.5 Plot error versus track error

Finally, we discuss the influence of the OBE presented in this chapter on the information presented to the operator.

The errors calculated here represent the bearing error on a single reply of the transponder. A worst-case assumption is that the measurement error of a single reply is also the measurement error of the plot, i.e. the reported MSSR measurement. In case a plot is derived from multiple replies per dwell, which is generally the case, the measurement error of the plot will be less than the measurement error of a single reply. A tracker processes plots messages and presents track updates of targets on a computer screen to the operator. In general, the error in a plot is also not the same as the error in a track update. Especially when a target does not manoeuvre, positional errors in plots will be ‘smoothed’ by the track algorithm.

4.5 Mitigation by other MSSR

The DEA of the MSSR shows that wind turbines within the surveillance area introduce some degradation, expressed as an increased OBE for targets across the instrumented range and at various altitudes. These performance losses indicate that the wind turbines could potentially interfere with the precision of the MSSR in specific areas. To assess potential mitigation, the coverage of a second en-route Mode-S MSSR in the region, the combined PSR and MSSR Tooman, was estimated under the assumption of an undisturbed environment (i.e., assuming that there are no wind turbines in Line-of-Sight of the MSSR). The radar parameters that are relevant for this analysis are presented in Table 3.5. Note that the coordinates provided by Ai Bridges [3] are slightly different compared to the location on satellite images see Figure 4.26, however, this will not affect the results.

Figure 4.26 The combined PSR and en-route MSSR at Tooman Hill housed in a radome. Note that the provided coordinates are slightly off (Image from Google Earth).

Table 4.4 Relevant radar parameters of the combined PSR & Mode-S MSSR Tooman [3].

Parameter	Value
Antenna position	Stand-alone
X (UTM29N)	519760 E
Y (UTM29N)	5841280 N
Latitude (WGS84)	53.555556° N
Longitude (WGS84)	6.250833° W
Height (EGM96)	31 m AGL
	156 m AMSL
Number of elements	35 m
Antenna length	8.5 m
Frequency	1090 MHz
Maximum Instrumented Range	256 NM

The Line-of-Sight coverage diagrams are shown for targets at altitudes of 5000, 7000, 10000 and 35000 ft in Figure 4.27, Figure 4.28, Figure 4.29 and Figure 4.30, respectively. These figures show that the second MSSR provides overlapping coverage with the first MSSR system in the sectors affected by the consented and newly planned wind turbines. Consequently, the second MSSR can serve as an effective redundant system, ensuring continued surveillance performance and operational robustness in areas where the MSSR at Woodcock Hill experiences reduced performance.

Note that there are potentially even more existing MSSRs that provide coverage in the affected areas of Woodcock Hill, such as the combined PSR and MSSR at Dublin International Airport. This is currently out of the scope of this study.

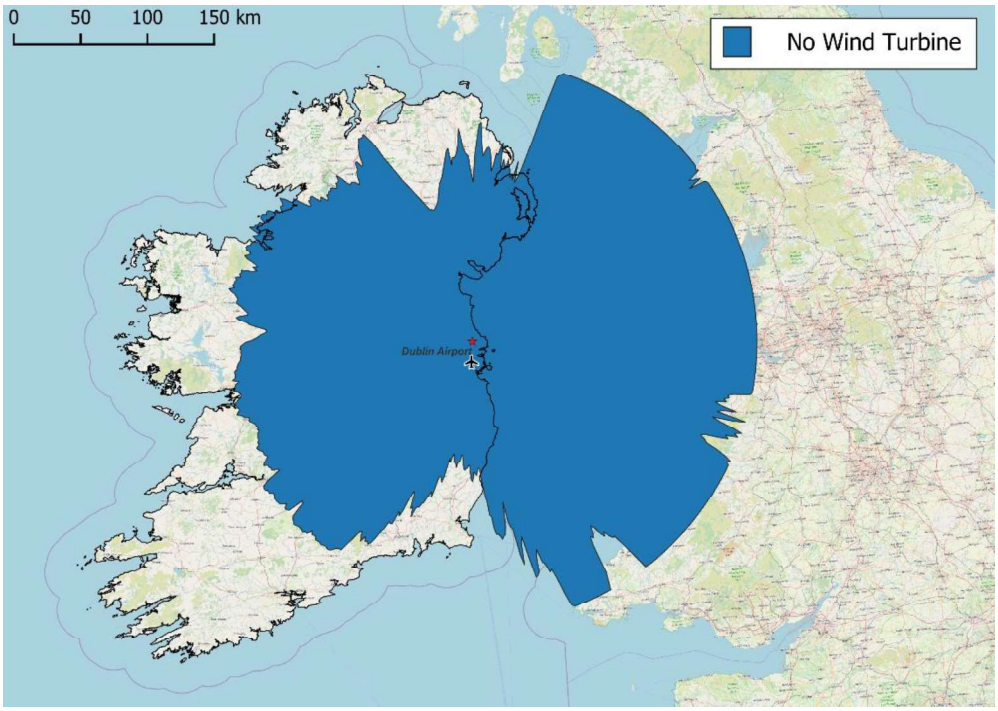

Figure 4.27 Line-of-Sight coverage diagram for a target at 5000 ft AMSL as seen from a secondary MSSR. No wind turbines are taken into account.

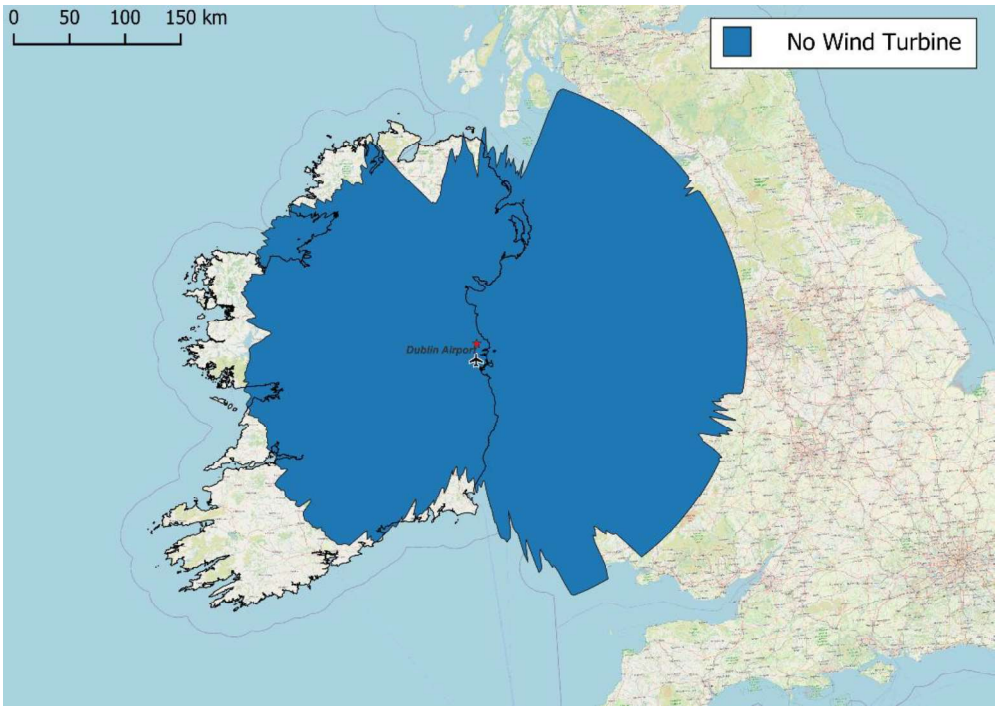

Figure 4.28 Line-of-Sight coverage diagram for a target at 7000 ft AMSL as seen from a secondary MSSR. No wind turbines are taken into account.

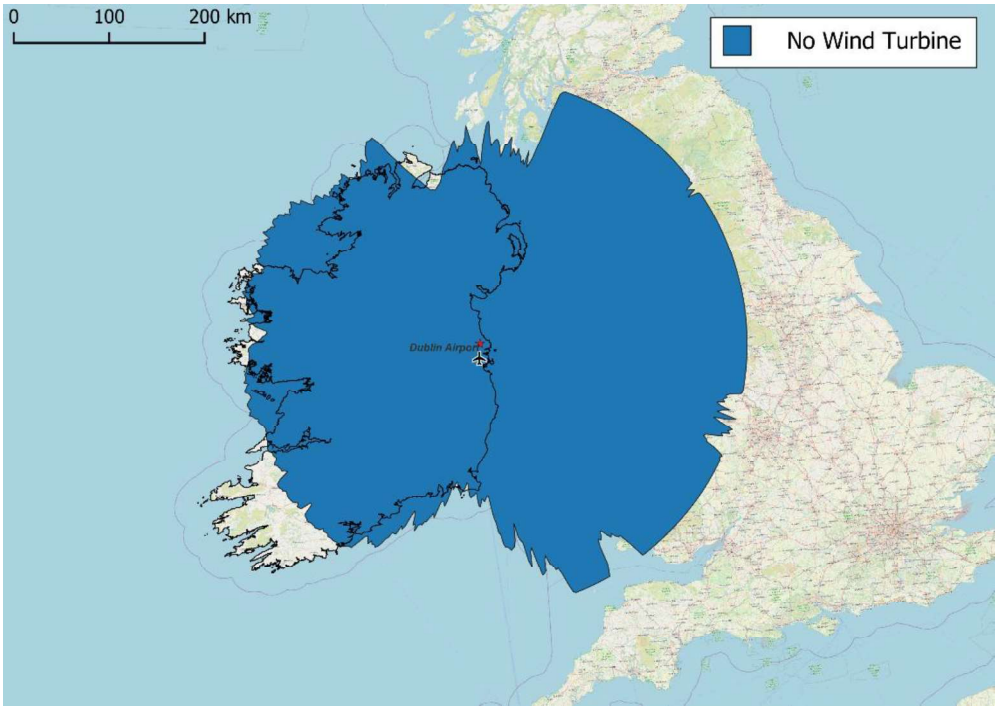

Figure 4.29 Line-of-Sight coverage diagram for a target at 10000 ft AMSL as seen from a secondary MSSR. No wind turbines are taken into account.

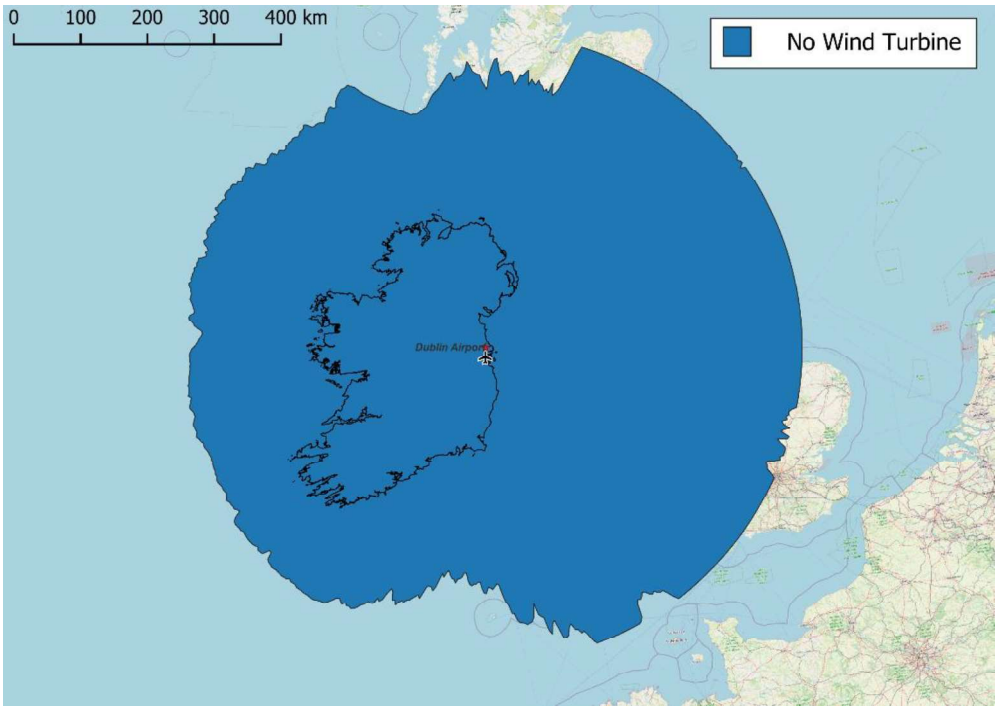

Figure 4.30 Line-of-Sight coverage diagram for a target at 35000 ft AMSL as seen from a secondary MSSR. No wind turbines are taken into account.

5 Conclusions

The consented planned wind turbines that have been included in the simulations, have an effect on the MSSR in an azimuth sector of 39°, from 26° to 65°. When the newly planned wind turbines at Ballycar are added, a zone of additional performance loss at an azimuth range of approximately 40°, from 70° to 110° as seen from the radar, is present.

The secondary radar has Line-of-Sight to all wind turbines (see Sections 4.1 and 4.2). The regions where the turbines have an effect on the radar are dependent on the target height and are displayed in Section 4.3. From this, it can be observed that both situations, with and without the newly planned wind turbines at Ballycar, there could be an effect on the MSSR performance due to the newly planned wind turbines when the target is at a certain area.

The maximum absolute OBE that could occur due to the newly planned turbines at Ballycar differ based on the target height. At lower target height, the so-called orange area, where the boresight measurement is interfered by the mast and nacelle, the maximum absolute off-boresight error is found to be 0.45°. At higher target heights, the so-called red area, where the boresight measurement is interfered by only the blade standing in the upright position, the absolute off-boresight error equals 0.44°. The 1σ standard deviation value measures 0.191° for the orange area and 0.134° for the red area. It has been shown that after the newly planned wind turbines are built, the change in the expected cross-range error due to these wind turbines is negligible small.

At last, is has been shown that another existing MSSR (i.e., MSSR Tooman) could provide overlapping coverage in the sectors affected by the consented and newly planned wind turbines, ensuring redundancy and maintaining surveillance performance where the Woodcock Hill MSSR shows reduced performance.

6 Bibliography

[1] EUROCONTROL, *Guidelines on How to Assess the Potential Impact of Wind Turbines on Surveillance Sensors (EUROCONTROL-GUID-0130),* 1.2 ed., 2014.

[2] L. Vinagre and K. Woodbridge, “Secondary surveillance radar monopulse target azimuth error estimation due to obstacle shadowing,” in *IEEE Radar Conference. Radar into the Next Millennium (Cat. No.99CH36249)*, Waltham, MA, USA, 1999.

[3] Ai Bridges Limited, *Radar details with coordinates and heights primary and secondary radars in Ireland,* 2025 November 12.

Defence, Safety & Security

Oude Waalsdorperweg 63
2597 AK Den Haag
www.tno.nl

TNO innovation for life